# LMH2100 50 MHz to 4 GHz 40 dB Logarithmic Power Detector for CDMA and WCDMA

**Check for Samples: LMH2100**

## FEATURES

- **40 dB Linear in dB Power Detection Range**
- **Output Voltage Range 0.3 to 2V**
- **Shutdown**
- **Multi-Band Operation from 50 MHz to 4 GHz**
- **0.5 dB Accurate Temperature Compensation**
- **External Configurable Output Filter Bandwidth**
- **0.4 mm-Pitch DSBGA Package**

## APPLICATIONS

- **UMTS/CDMA/WCDMA RF Power Control**
- **GSM/GPRS RF Power Control**
- **PA Modules**
- **IEEE 802.11b, g (WLAN)**

## DESCRIPTION

The LMH2100 is a 40 dB RF power detector intended for use in CDMA and WCDMA applications. The device has an RF frequency range from 50 MHz to 4 GHz. It provides an accurate temperature and supply compensated output voltage that relates linearly to the RF input power in dBm. The circuit operates with a single supply from 2.7V to 3.3V.

The LMH2100 has an RF power detection range from −45 dBm to −5 dBm and is ideally suited for direct use in combination with a 30 dB directional coupler. Additional low-pass filtering of the output signal can be realized by means of an external resistor and capacitor. Figure 1 shows a detector with an additional output low pass filter. The filter frequency is set with $R_S$ and $C_S$.

Figure 2 shows a detector with an additional feedback low pass filter. Resistor $R_P$ is optional and will lower the Trans impedance gain ($R_{TRANS}$). The filter frequency is set with $C_P//C_{TRANS}$ and $R_P//R_{TRANS}$.

The device is active for Enable = High, otherwise it is in a low power consumption shutdown mode. To save power and prevent discharge of an external filter capacitance, the output (OUT) is high-impedance during shutdown.

The LMH2100 power detector is offered in the small 0.4 mm pitch DSBGA package.

### Typical Application

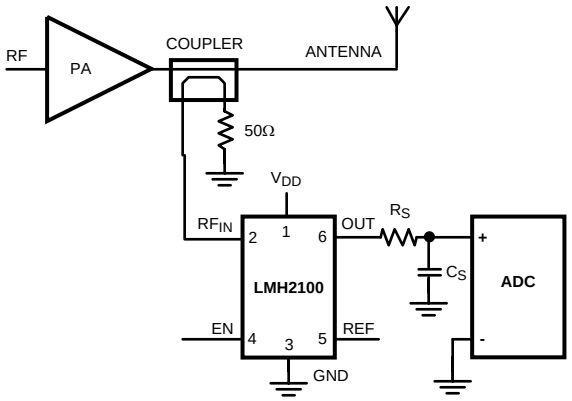


**Figure 1. LMH2100 with Output RC Low Pass Filter**

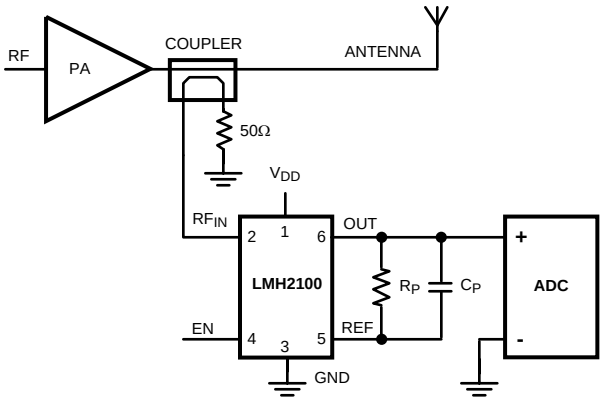


**Figure 2. LMH2100 with Feedback (R)C Low Pass Filter**

These devices have limited built-in ESD protection. The leads should be shorted together or the device placed in conductive foam during storage or handling to prevent electrostatic damage to the MOS gates.

## Absolute Maximum Ratings (1)(2)

| | |
|---|---|
| Supply Voltage | |
| $V_{DD}$ - GND | 3.6V |
| RF Input | |
| Input power | 10 dBm |
| DC Voltage | 400 mV |
| Enable Input Voltage | $V_{SS}$ - 0.4V < $V_{EN}$ < $V_{DD}$ + 0.4V |
| ESD Tolerance (3) | |
| Human Body Model | 2000V |
| Machine Model | 200V |
| Charge Device Model | 2000V |
| Storage Temperature Range | −65°C to 150°C |
| Junction Temperature (4) | 150°C |
| Maximum Lead Temperature | |
| (Soldering,10 sec) | 260°C |

(1) Absolute Maximum Ratings indicate limits beyond which damage to the device may occur. Operating Ratings indicate conditions for which the device is intended to be functional, but specific performance is not ensured. For ensured specifications and the test conditions, see the 2.7 V DC and AC Electrical Characteristics.
(2) If Military/Aerospace specified devices are required, please contact the Texas Instruments Sales Office/ Distributors for availability and specifications.
(3) Human body model, applicable std. MIL-STD-883, Method 3015.7. Machine model, applicable std. JESD22–A115–A (ESD MM std of JEDEC). Field-Induced Charge-Device Model, applicable std. JESD22–C101–C. (ESD FICDM std. of JEDEC)
(4) The maximum power dissipation is a function of $T_{J(MAX)}$ , $\theta_{JA}$. The maximum allowable power dissipation at any ambient temperature is $P_D = (T_{J(MAX)} - T_A)/\theta_{JA}$. All numbers apply for packages soldered directly into a PC board.

## Operating Ratings (1)

| | |
|---|---|
| Supply Voltage | 2.7V to 3.3V |
| Temperature Range | −40°C to +85°C |
| RF Frequency Range | 50 MHz to 4 GHz |
| RF Input Power Range (2) | −45 dBm to −5 dBm<br>−58 dBV to −18 dBV |
| Package Thermal Resistance $\theta_{JA}$ (3) | 126.3°C/W |

(1) Absolute Maximum Ratings indicate limits beyond which damage to the device may occur. Operating Ratings indicate conditions for which the device is intended to be functional, but specific performance is not ensured. For ensured specifications and the test conditions, see the 2.7 V DC and AC Electrical Characteristics.
(2) Power in dBV = dBm + 13 when the impedance is 50Ω.
(3) The maximum power dissipation is a function of $T_{J(MAX)}$ , $\theta_{JA}$. The maximum allowable power dissipation at any ambient temperature is $P_D = (T_{J(MAX)} - T_A)/\theta_{JA}$. All numbers apply for packages soldered directly into a PC board.

## 2.7 V DC and AC Electrical Characteristics

Unless otherwise specified, all limits are ensured at $T_A$ = 25°C, $V_{DD}$ = 2.7V, RF input frequency f = 1855 MHz CW (Continuous Wave, unmodulated). **Boldface** limits apply at the temperature extremes (1).

| Symbol | Parameter | Condition | Min (2) | Typ (3) | Max (2) | Units |
|---|---|---|---|---|---|---|
| **Supply Interface** | | | | | | |
| $I_{DD}$ | Supply Current | Active mode: EN = High, no signal present at $RF_{IN}$. | 6.3<br>**5.0** | 7.1 | 7.9<br>**9.2** | mA |
| | | Shutdown: EN = Low, no signal present at $RF_{IN}$. | | 0.5 | 0.9<br>**1.9** | µA |
| | | EN = Low: $P_{IN}$ = 0 dBm (4) | | | **10** | |
| **Logic Enable Interface** | | | | | | |
| $V_{LOW}$ | EN Logic Low Input Level (Shutdown Mode) | | | | **0.6** | V |
| $V_{HIGH}$ | EN Logic High Input Level | | **1.1** | | | V |
| $I_{EN}$ | Current into EN Pin | | | | **50** | nA |
| **RF Input Interface** | | | | | | |
| $R_{IN}$ | Input Resistance | | 46.7 | 51.5 | 56.4 | Ω |
| **Output Interface** | | | | | | |
| $V_{OUT}$ | Output Voltage Swing | From Positive Rail, Sourcing, $V_{REF}$ = 0V, $I_{OUT}$ = 1 mA | | 15.3 | 23.9<br>**28.9** | mV |
| | | From Negative Rail, Sinking, $V_{REF}$ = 2.7V, $I_{OUT}$ = 1 mA | | 13.1 | 22.3<br>**28.3** | |
| $I_{OUT}$ | Output Short Circuit Current | Sourcing, $V_{REF}$ = 0V, $V_{OUT}$ = 2.6V | 5.8<br>**5.2** | 7.3 | | mA |
| | | Sinking, $V_{REF}$ = 2.7V, $V_{OUT}$ = 0.1V | 6.2<br>**5.4** | 8.3 | | |
| BW | Small Signal Bandwidth | No RF input signal. Measured from REF input current to $V_{OUT}$ | | 416 | | kHz |
| $R_{TRANS}$ | Output Amp Transimpedance Gain | No RF input signal, from $I_{REF}$ to $V_{OUT}$, DC | 40.7 | 43.3 | 46.7 | kΩ |
| SR | Slew Rate | Positive, $V_{REF}$ from 2.7V to 0V | 3.4<br>**3.3** | 3.9 | | V/µs |
| | | Negative, $V_{REF}$ from 0V to 2.7V | 3.8<br>**3.7** | 4.4 | | |
| $R_{OUT}$ | Output Impedance (4) | No RF input signal, EN = High. DC measurement | | 0.2 | 1.8<br>**4.0** | Ω |
| $I_{OUT,SD}$ | Output Leakage Current in Shutdown mode | EN = Low, $V_{OUT}$ = 2.0V | | | **100** | nA |
| **RF Detector Transfer** | | | | | | |
| $V_{OUT,MAX}$ | Maximum Output Voltage $P_{IN}$= −5 dBm (4) | f = 50 MHz | **1.69** | 1.77 | **1.82** | V |
| | | f = 900 MHz | **1.67** | 1.78 | **1.83** | |
| | | f = 1855 MHz | **1.57** | 1.65 | **1.70** | |
| | | f = 2500 MHz | **1.47** | 1.55 | **1.60** | |
| | | f = 3000 MHz | **1.38** | 1.46 | **1.51** | |
| | | f = 3500 MHz | **1.25** | 1.34 | **1.40** | |
| | | f = 4000 MHz | **1.16** | 1.25 | **1.30** | |

(1) Electrical Table values apply only for factory testing conditions at the temperature indicated. Factory testing conditions result in very limited self-heating of the device such that $T_J = T_A$. No specification of parametric performance is indicated in the electrical tables under conditions of internal self-heating where $T_J > T_A$.
(2) All limits are ensured by test or statistical analysis.
(3) Typical values represent the most likely parametric norm as determined at the time of characterization. Actual typical values may vary over time and will also depend on the application and configuration. The typical values are not tested and are not specified on shipped production material.
(4) All limits are ensured by design and measurements which are performed on a limited number of samples. Limits represent the mean ±3–sigma values. The typical value represents the statistical mean value.

## 2.7 V DC and AC Electrical Characteristics (continued)

Unless otherwise specified, all limits are ensured at $T_A$ = 25°C, $V_{DD}$ = 2.7V, RF input frequency f = 1855 MHz CW (Continuous Wave, unmodulated). **Boldface** limits apply at the temperature extremes (1).

| Symbol | Parameter | Condition | Min (2) | Typ (3) | Max (2) | Units |
|---|---|---|---|---|---|---|
| $V_{OUT,MIN}$ | Minimum Output Voltage (Pedestal) | No input signal | 207<br>**173** | 266 | 324<br>**365** | mV |
| $\Delta V_{OUT}$ | Output Voltage Range $P_{IN}$ from −45 dBm to −5 dBm (4) | f = 50 MHz | **1.38** | 1.44 | **1.49** | V |
| | | f = 900 MHz | **1.34** | 1.43 | **1.46** | |
| | | f = 1855 MHz | **1.27** | 1.32 | **1.36** | |
| | | f = 2500 MHz | **1.19** | 1.23 | **1.27** | |
| | | f = 3000 MHz | **1.11** | 1.16 | **1.19** | |
| | | f = 3500 MHz | **1.00** | 1.05 | **1.10** | |
| | | f = 4000 MHz | **0.91** | 0.97 | **1.01** | |
| $K_{SLOPE}$ | Logarithmic Slope (4) | f = 50 MHz | 39.6 | 40.9 | 42.1 | mV/dB |
| | | f = 900 MHz | 37.0 | 38.2 | 39.4 | |
| | | f = 1855 MHz | 34.5 | 35.5 | 36.5 | |
| | | f = 2500 MHz | 32.7 | 33.7 | 34.6 | |
| | | f = 3000 MHz | 31.1 | 32.1 | 33.1 | |
| | | f = 3500 MHz | 29.7 | 30.7 | 31.6 | |
| | | f = 4000 MHz | 28.5 | 29.4 | 30.3 | |
| $P_{INT}$ | Logarithmic Intercept (4) | f = 50 MHz | –50.2 | −49.5 | –48.8 | dBm |
| | | f = 900 MHz | –53.6 | −52.7 | –51.8 | |
| | | f = 1855 MHz | –53.2 | −52.3 | –51.4 | |
| | | f = 2500 MHz | –52.4 | −51.2 | –50.1 | |
| | | f = 3000 MHz | –51.2 | −50.1 | –48.9 | |
| | | f = 3500 MHz | –49.1 | −47.8 | –46.4 | |
| | | f = 4000 MHz | –47.3 | −46.1 | –44.9 | |
| $t_{ON}$ | Turn-On Time | No signal at $P_{IN}$, Low-High transition EN. $V_{OUT}$ to 90% | | 8.2 | 9.8<br>**12.0** | µs |
| $t_R$ | Rise Time (5) | $P_{IN}$ = No signal to 0 dBm, $V_{OUT}$ from 10% to 90% | | 2 | **12** | µs |
| $t_F$ | Fall Time (5) | $P_{IN}$ = 0 dBm to no signal, $V_{OUT}$ from 90% to 10% | | 2 | **12** | µs |
| $e_n$ | Output Referred Noise (5) | $P_{IN}$ = −10 dBm, at 10 kHz | | 1.5 | | µV/√Hz |
| $v_N$ | Output Referred Noise (6) | Integrated over frequency band 1 kHz - 6.5 kHz | | 100 | **150** | $\mu V_{RMS}$ |
| PSRR | Power Supply Rejection Ratio (5) | $P_{IN}$ = −10 dBm, f = 1800 MHz | **55** | 60 | | dB |

(5) This parameter is ensured by design and/or characterization and is not tested in production.
(6) All limits are ensured by design and measurements which are performed on a limited number of samples. Limits represent the mean ±3–sigma values. The typical value represents the statistical mean value.

## 2.7 V DC and AC Electrical Characteristics (continued)

Unless otherwise specified, all limits are ensured at $T_A$ = 25°C, $V_{DD}$ = 2.7V, RF input frequency f = 1855 MHz CW (Continuous Wave, unmodulated). **Boldface** limits apply at the temperature extremes (1).

| Symbol | Parameter | Condition | Min (2) | Typ (3) | Max (2) | Units |
|---|---|---|---|---|---|---|
| **Power Measurement Performance** | | | | | | |
| $E_{LC}$ | Log Conformance Error (7)<br>−40 dBm ≤ $P_{IN}$ ≤ −10 dBm | f = 50 MHz | -0.2<br>**-0.8** | 0.12 | 1.2<br>**1.3** | dB |
| | | f = 900 MHz | -0.4<br>**-1.0** | -0.06 | 0.2<br>**0.3** | |
| | | f = 1855 MHz | -0.3<br>**-0.7** | -0.03 | 0.3<br>**0.4** | |
| | | f = 2500 MHz | -0.2<br>**-0.8** | 0.04 | 0.8<br>**1.1** | |
| | | f = 3000 MHz | -0.1<br>**1.0** | 0.13 | 1.6<br>**1.8** | |
| | | f = 3500 MHz | -0.036<br>**-1.0** | 0.35 | 3.3<br>**3.5** | |
| | | f = 4000 MHz | -0.048<br>**-1.0** | 0.65 | 4.6<br>**4.9** | |
| $E_{VOT}$ | Variation over Temperature (7)<br>−40 dBm ≤ $P_{IN}$ ≤ −10 dBm | f = 50 MHz | **-0.63** | | **0.43** | dB |
| | | f = 900 MHz | **-0.94** | | **0.30** | |
| | | f = 1855 MHz | **-0.71** | | **0.33** | |
| | | f = 2500 MHz | **-0.88** | | **0.35** | |
| | | f = 3000 MHz | **-1.03** | | **0.37** | |
| | | f = 3500 MHz | **-1.10** | | **0.33** | |
| | | f = 4000 MHz | **-1.12** | | **0.33** | |
| $E_{1\ dB}$ | Measurement Error for a 1 dB Input Power Step (7)<br>−40 dBm ≤ $P_{IN}$ ≤ −10 dBm | f = 50 MHz | **-0.064** | | **0.066** | dB |
| | | f = 900 MHz | **-0.123** | | **0.051** | |
| | | f = 1855 MHz | **-0.050** | | **0.067** | |
| | | f = 2500 MHz | **-0.058** | | **0.074** | |
| | | f = 3000 MHz | **-0.066** | | **0.069** | |
| | | f = 3500 MHz | **-0.082** | | **0.066** | |
| | | f = 4000 MHz | **-0.098** | | **0.072** | |
| $E_{10\ dB}$ | Measurement Error for a 10 dB Input Power Step (7)<br>−40 dBm ≤ $P_{IN}$ ≤ −10 dBm | f = 50 MHz | **-0.40** | | **0.27** | dB |
| | | f = 900 MHz | **-0.58** | | **0.22** | |
| | | f = 1855 MHz | **-0.29** | | **0.20** | |
| | | f = 2500 MHz | **-0.28** | | **0.24** | |
| | | f = 3000 MHz | **-0.38** | | **0.29** | |
| | | f = 3500 MHz | **-0.60** | | **0.40** | |
| | | f = 4000 MHz | **-0.82** | | **0.43** | |
| $S_T$ | Temperature Sensitivity<br>−40°C < $T_A$ < 25°C (7)<br>−40 dBm ≤ $P_{IN}$ ≤ −10 dBm | f = 50 MHz | **-6.5** | | **8.6** | mdB/°C |
| | | f = 900 MHz | **-4.7** | | **14.5** | |
| | | f = 1855 MHz | **-5.1** | | **11.0** | |
| | | f = 2500 MHz | **-4.3** | | **13.6** | |
| | | f = 3000 MHz | **-1.5** | | **15.8** | |
| | | f = 3500 MHz | **0.1** | | **16.9** | |
| | | f = 4000 MHz | **0.5** | | **17.3** | |

(7) All limits are ensured by design and measurements which are performed on a limited number of samples. Limits represent the mean ±3–sigma values. The typical value represents the statistical mean value.

## 2.7 V DC and AC Electrical Characteristics (continued)

Unless otherwise specified, all limits are ensured at $T_A$ = 25°C, $V_{DD}$ = 2.7V, RF input frequency f = 1855 MHz CW (Continuous Wave, unmodulated). **Boldface** limits apply at the temperature extremes (1).

| Symbol | Parameter | Condition | Min (2) | Typ (3) | Max (2) | Units |
|---|---|---|---|---|---|---|
| $S_T$ | Temperature Sensitivity 25°C < $T_A$ < 85°C (7) −40 dBm ≤ $P_{IN}$ ≤ −10 dBm | f = 50 MHz | **-10.5** | | **0.5** | mdB/°C |
| | | f = 900 MHz | **-10.5** | | **2.6** | |
| | | f = 1855 MHz | **-11.3** | | **3.4** | |
| | | f = 2500 MHz | **-10.6** | | **5.8** | |
| | | f = 3000 MHz | **-11.2** | | **6.1** | |
| | | f = 3500 MHz | **-12.9** | | **5.5** | |
| | | f = 4000 MHz | **-17.8** | | **5.5** | |
| $S_T$ | Temperature Sensitivity −40°C < $T_A$ < 25°C, (7) $P_{IN}$ = −10 dBm | f = 50 MHz | **-5.4** | | **8.6** | mdB/°C |
| | | f = 900 MHz | **0.3** | | **14.5** | |
| | | f = 1855 MHz | **-3.1** | | **11.0** | |
| | | f = 2500 MHz | **-1.6** | | **13.6** | |
| | | f = 3000 MHz | **0.9** | | **15.8** | |
| | | f = 3500 MHz | **2.5** | | **16.9** | |
| | | f = 4000 MHz | **2.7** | | **17.3** | |
| $S_T$ | Temperature Sensitivity 25°C < $T_A$ < 85°C, (7) $P_{IN}$ = −10 dBm | f = 50 MHz | **-10.5** | | **0.5** | mdB/°C |
| | | f = 900 MHz | **-10.5** | | **2.6** | |
| | | f = 1855 MHz | **-11.3** | | **3.3** | |
| | | f = 2500 MHz | **-10.6** | | **5.4** | |
| | | f = 3000 MHz | **-11.2** | | **6.1** | |
| | | f = 3500 MHz | **-12.9** | | **4.4** | |
| | | f = 4000 MHz | **-17.8** | | **-1.1** | |
| $P_{MAX}$ | Maximum Input Power for $E_{LC}$ = 1 dB (8) | f = 50 MHz | **-9.2** | -7.4 | | dBm |
| | | f = 900 MHz | **-10.5** | -8.6 | | |
| | | f = 1855 MHz | **-8.2** | -6.5 | | |
| | | f = 2500 MHz | **-7.3** | -5.6 | | |
| | | f = 3000 MHz | **-6.3** | -4.4 | | |
| | | f = 3500 MHz | **-6.9** | -1.9 | | |
| | | f = 4000 MHz | **-11.1** | -7.2 | | |
| $P_{MIN}$ | Minimum Input Power for $E_{LC}$ = 1 dB (8) | f = 50 MHz | | -38.9 | **-38.1** | dBm |
| | | f = 900 MHz | | -43.1 | **-42.3** | |
| | | f = 1855 MHz | | -42.2 | **-41.0** | |
| | | f = 2500 MHz | | -40.6 | **-38.9** | |
| | | f = 3000 MHz | | -38.7 | **-37.0** | |
| | | f = 3500 MHz | | -35.9 | **-34.7** | |
| | | f = 4000 MHz | | -33.5 | **-32.0** | |
| DR | Dynamic Range for $E_{LC}$ = 1 dB (8) | f = 50 MHz | **29.5** | 31.6 | | dB |
| | | f = 900 MHz | **33.3** | 35.2 | | |
| | | f = 1855 MHz | **34.2** | 36.5 | | |
| | | f = 2500 MHz | **34.1** | 36.1 | | |
| | | f = 3000 MHz | **33.4** | 35.5 | | |
| | | f = 3500 MHz | **28.5** | 35.1 | | |
| | | f = 4000 MHz | **22.7** | 26.3 | | |

(8) All limits are ensured by design and measurements which are performed on a limited number of samples. Limits represent the mean ±3–sigma values. The typical value represents the statistical mean value.

## CONNECTION DIAGRAM

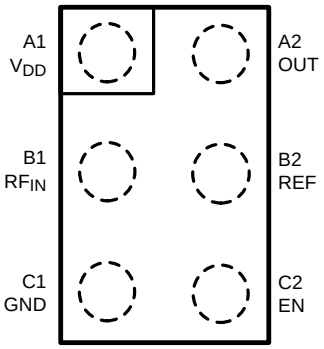


**Figure 3. 6-Bump DSBGA**
**Top View**

## PIN DESCRIPTIONS

| | DSBGA | Name | Description |
|---|---|---|---|
| Power Supply | A1 | $V_{DD}$ | Positive Supply Voltage |
| | C1 | GND | Power Ground |
| Logic Input | C2 | EN | The device is enabled for EN = High, and brought to a low-power shutdown mode for EN = Low. |
| Analog Input | B1 | $RF_{IN}$ | RF input signal to the detector, internally terminated with 50Ω. |
| Output | B2 | REF | Reference output, for differential output measurement (without pedestal). Connected to inverting input of output amplifier. |
| | A2 | OUT | Ground referenced detector output voltage (linear in dB) |

## BLOCK DIAGRAM

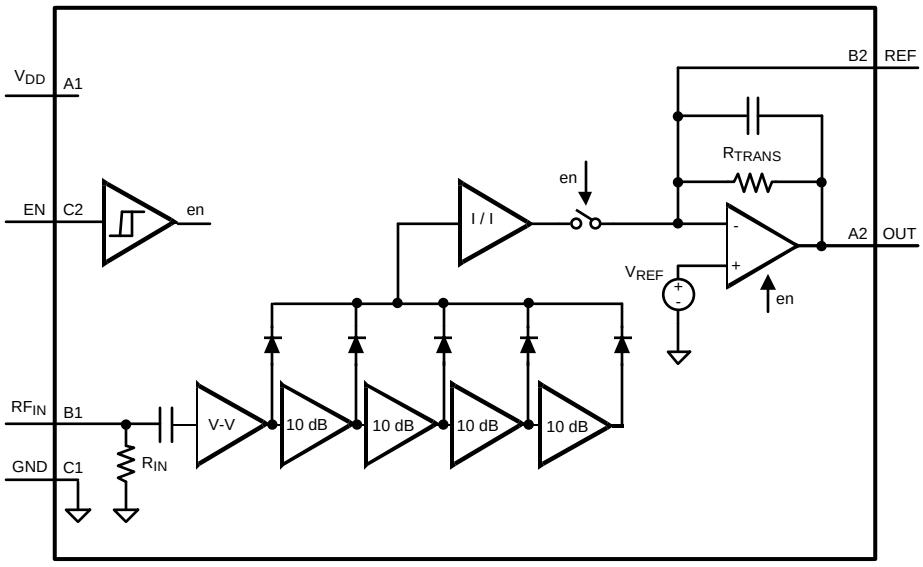


**Figure 4. LMH2100**

## Typical Performance Characteristics

Unless otherwise specified, $V_{DD}$ = 2.7V, $T_A$ = 25°C, measured on a limited number of samples.

**Supply Current vs. Supply Voltage**

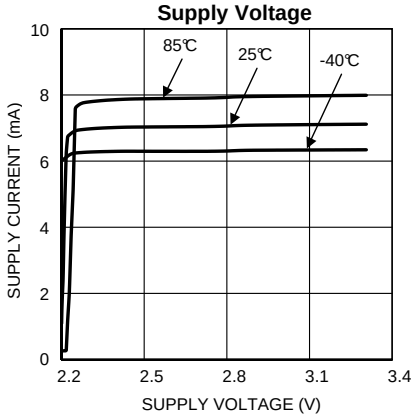


**Figure 5.**

**Supply Current vs. Enable Voltage**

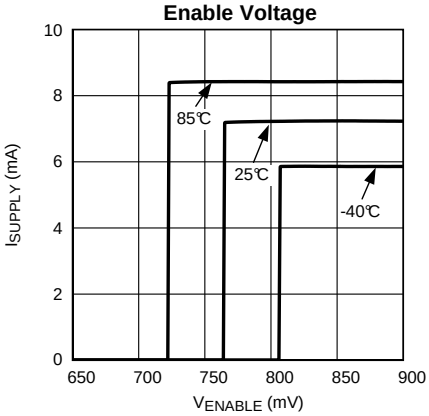


**Figure 6.**

**Output Voltage vs. RF input Power**

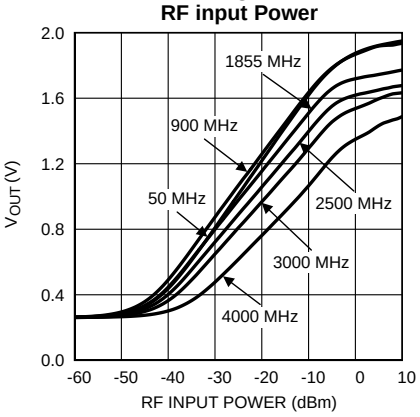


**Figure 7.**

**Log Slope vs. Frequency**

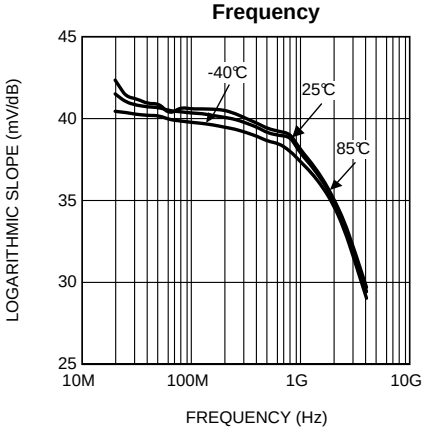


**Figure 8.**

**Log Intercept vs. Frequency**

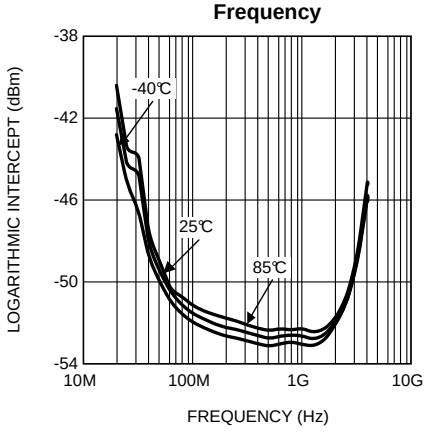


**Figure 9.**

**Output Voltage vs. Frequency**

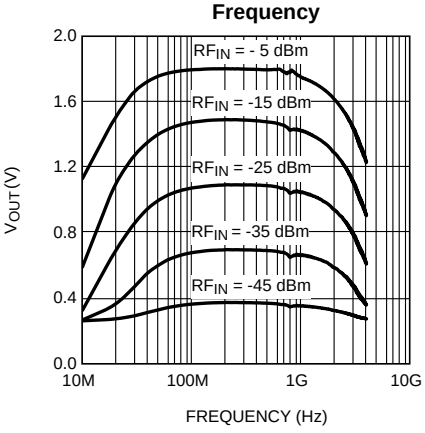


**Figure 10.**

## Typical Performance Characteristics (continued)

Unless otherwise specified, $V_{DD}$ = 2.7V, $T_A$ = 25°C, measured on a limited number of samples.

**Mean Output Voltage and Log Conformance Error vs. RF Input Power at 50 MHz**

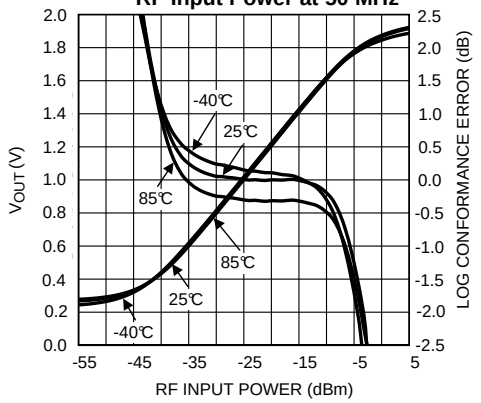


**Figure 11.**

**Mean Output Voltage and Log Conformance Error vs. RF Input Power at 900 MHz**

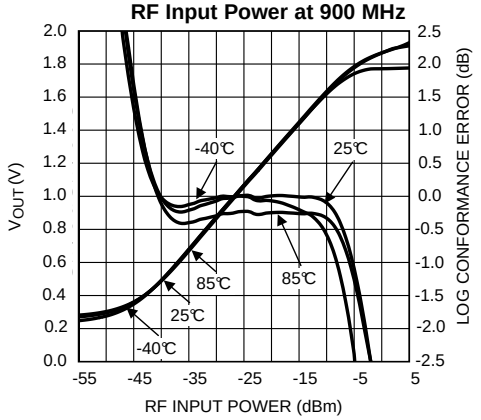


**Figure 12.**

**Mean Output Voltage and Log Conformance Error vs. RF Input Power at 1855 MHz**

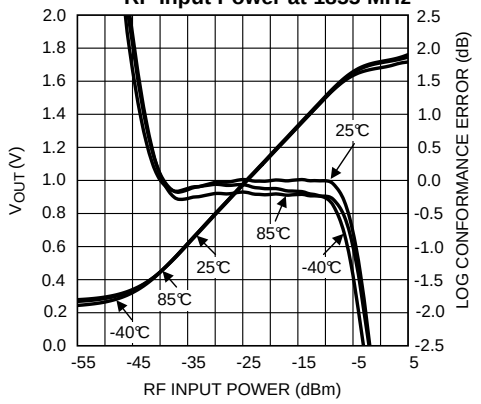


**Figure 13.**

**Mean Output Voltage and Log Conformance Error vs. RF Input Power at 2500 MHz**

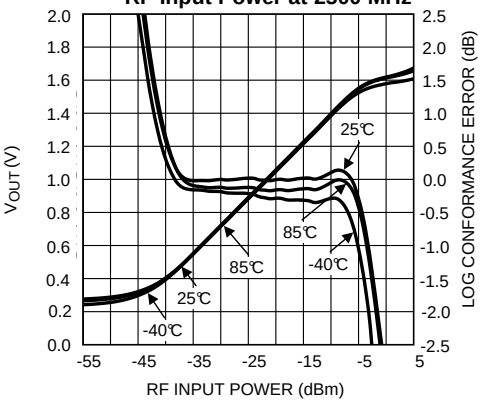


**Figure 14.**

**Mean Output Voltage and Log Conformance Error vs. RF Input Power at 3000 MHz**

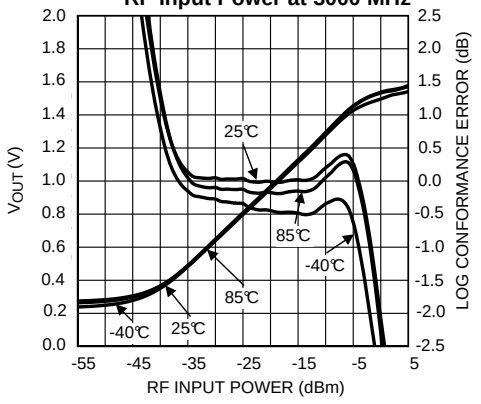


**Figure 15.**

**Mean Output Voltage and Log Conformance Error vs. RF Input Power at 3500 MHz**

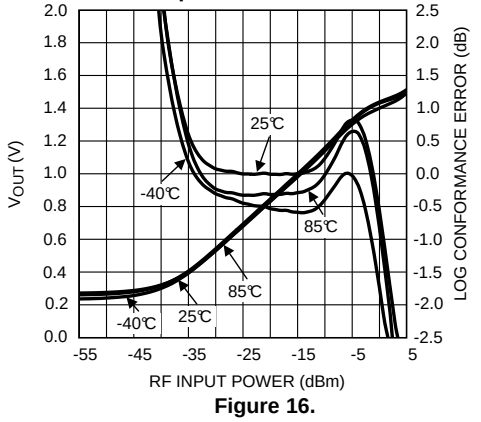


**Figure 16.**

## Typical Performance Characteristics (continued)

Unless otherwise specified, $V_{DD}$ = 2.7V, $T_A$ = 25°C, measured on a limited number of samples.

**Mean Output Voltage and Log Conformance Error vs. RF Input Power at 4000 MHz**

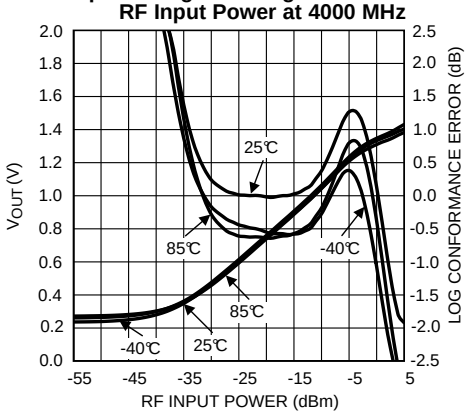


**Figure 17.**

**Log Conformance Error (Mean ±3 sigma) vs. RF Input Power at 50 MHz**

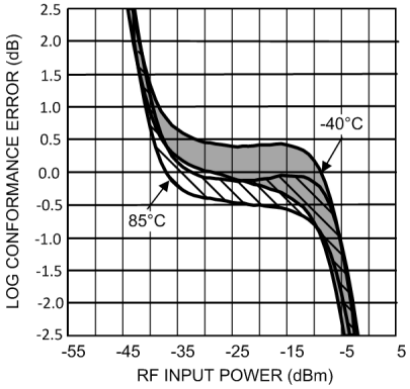


**Figure 18.**

**Log Conformance Error (Mean ±3 sigma) vs. RF Input Power at 900 MHz**

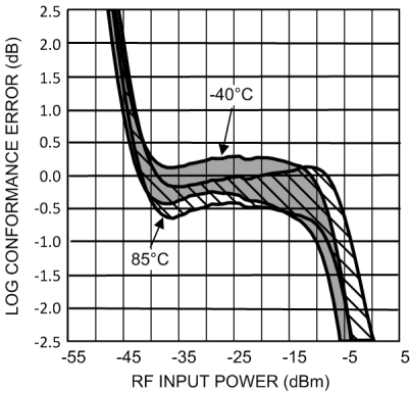


**Figure 19.**

**Log Conformance Error (Mean ±3 sigma) vs. RF Input Power at 1855 MHz**

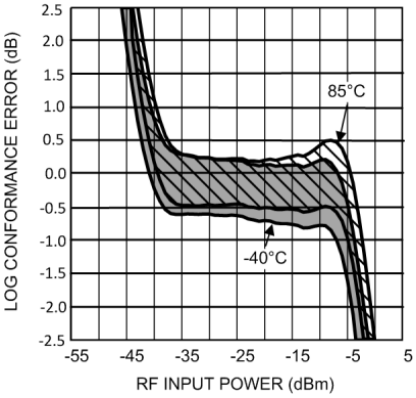


**Figure 20.**

**Log Conformance Error (Mean ±3 sigma) vs. RF Input Power at 2500 MHz**

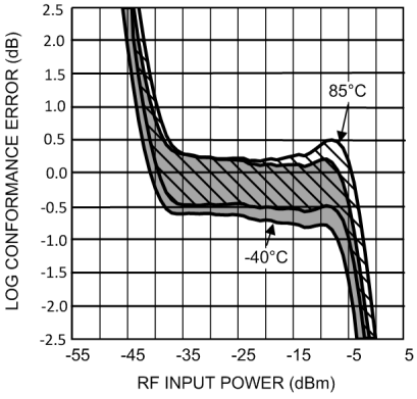


**Figure 21.**

**Log Conformance Error (Mean ±3 sigma) vs. RF Input Power at 3000 MHz**

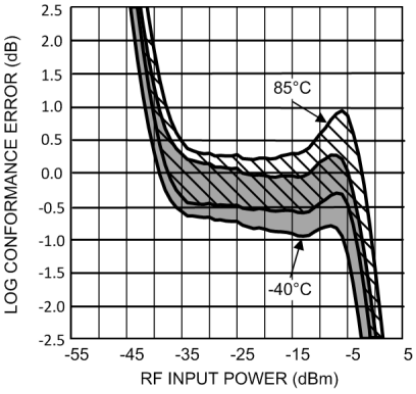


**Figure 22.**

## Typical Performance Characteristics (continued)

Unless otherwise specified, $V_{DD}$ = 2.7V, $T_A$ = 25°C, measured on a limited number of samples.

**Log Conformance Error (Mean ±3 sigma) vs. RF Input Power at 3500 MHz**

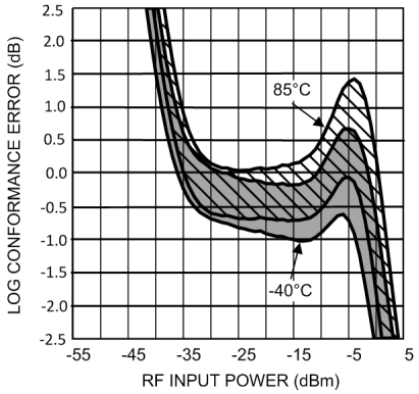


**Figure 23.**

**Log Conformance Error (Mean ±3 sigma) vs. RF Input Power at 4000 MHz**

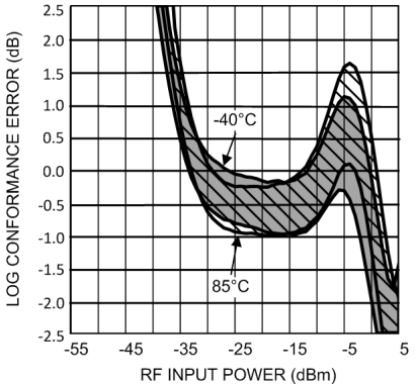


**Figure 24.**

**Mean Temperature Drift Error vs. RF Input Power at 50 MHz**

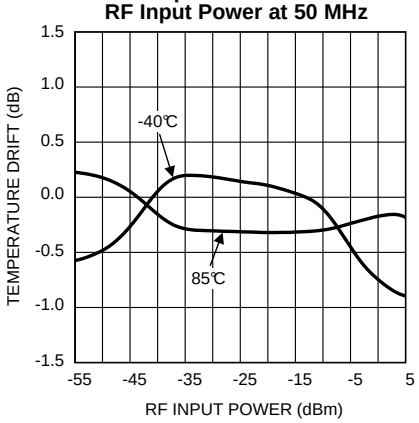


**Figure 25.**

**Mean Temperature Drift Error vs. RF Input Power at 900 MHz**

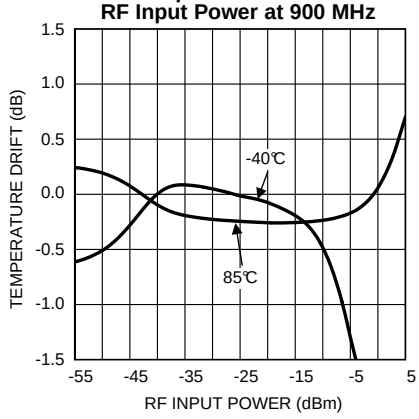


**Figure 26.**

**Mean Temperature Drift Error vs. RF Input Power at 1855 MHz**

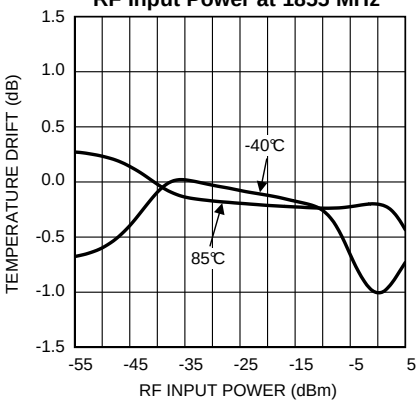


**Figure 27.**

**Mean Temperature Drift Error vs. RF Input Power at 2500 MHz**

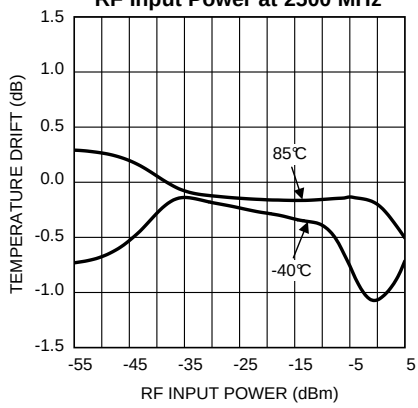


**Figure 28.**

## Typical Performance Characteristics (continued)

Unless otherwise specified, $V_{DD}$ = 2.7V, $T_A$ = 25°C, measured on a limited number of samples.

**Mean Temperature Drift Error vs. RF Input Power at 3000 MHz**

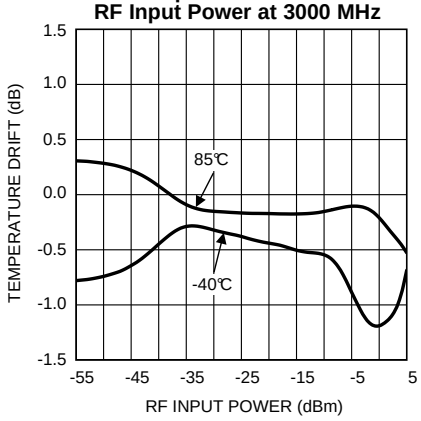


**Figure 29.**

**Mean Temperature Drift Error vs. RF Input Power at 3500 MHz**

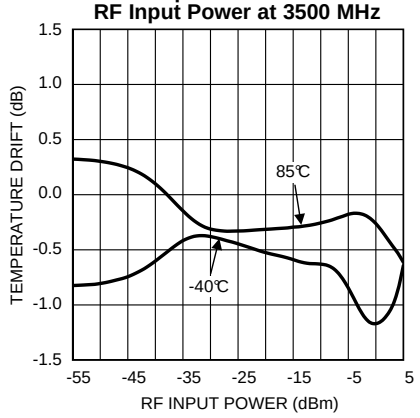


**Figure 30.**

**Mean Temperature Drift Error vs. RF Input Power at 4000 MHz**

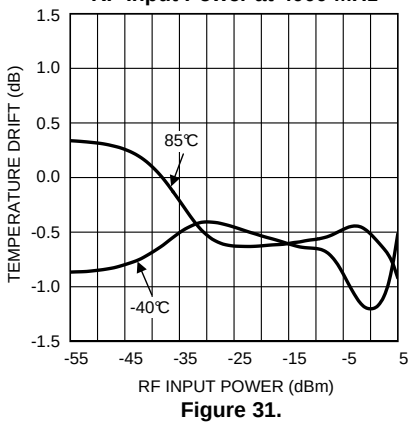


**Figure 31.**

**Temperature Drift Error (Mean ±3 sigma) vs. RF Input Power at 50 MHz**

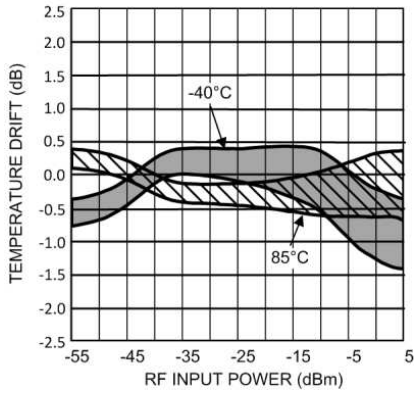


**Figure 32.**

**Temperature Drift Error (Mean ±3 sigma) vs. RF Input Power at 900 MHz**

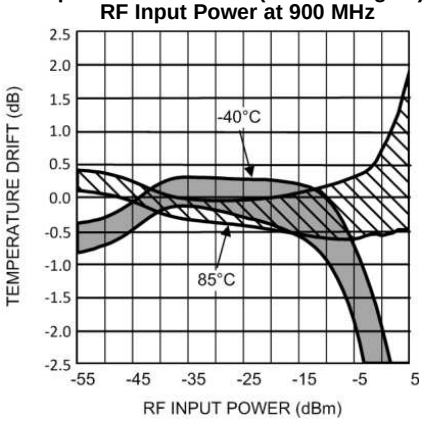


**Figure 33.**

**Temperature Drift Error (Mean ±3 sigma) vs. RF Input Power at 1855 MHz**

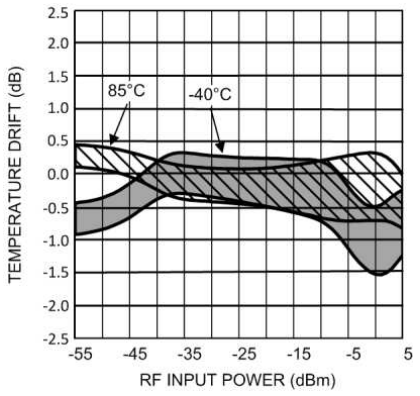


**Figure 34.**

## Typical Performance Characteristics (continued)

Unless otherwise specified, $V_{DD}$ = 2.7V, $T_A$ = 25°C, measured on a limited number of samples.

**Temperature Drift Error (Mean ±3 sigma) vs. RF Input Power at 2500 MHz**

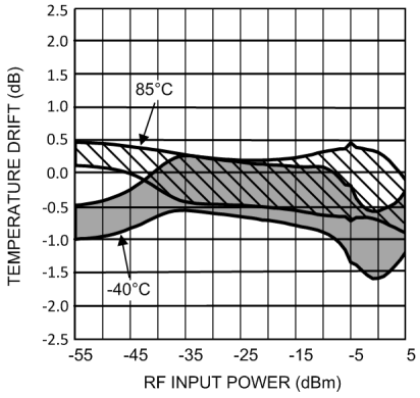


**Figure 35.**

**Temperature Drift Error (Mean ±3 sigma) vs. RF Input Power at 3000 MHz**

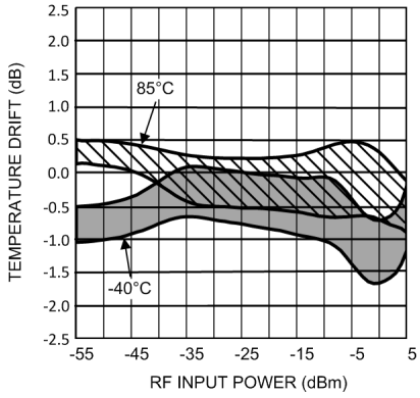


**Figure 36.**

**Temperature Drift Error (Mean ±3 sigma) vs. RF Input Power at 3500 MHz**

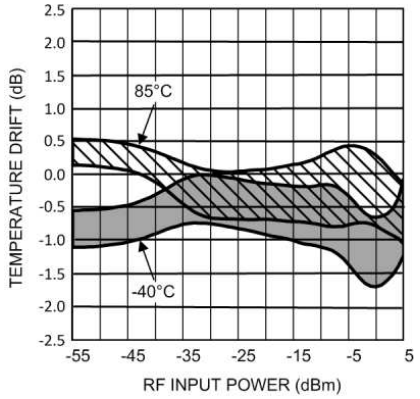


**Figure 37.**

**Temperature Drift Error (Mean ±3 sigma) vs. RF Input Power at 4000 MHz**

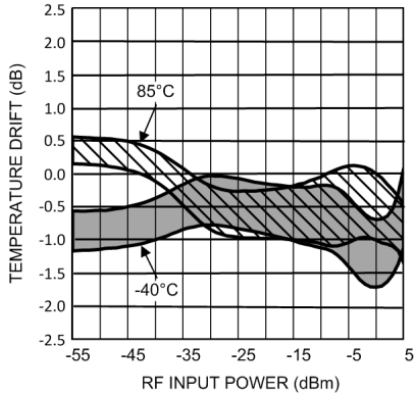


**Figure 38.**

**Error for 1 dB Input Power Step vs. RF Input Power at 50 MHz**

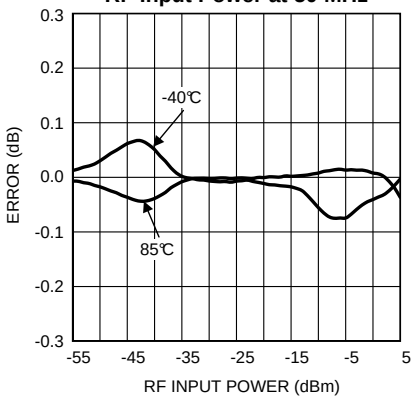


**Figure 39.**

**Error for 1 dB Input Power Step vs. RF Input Power at 900 MHz**

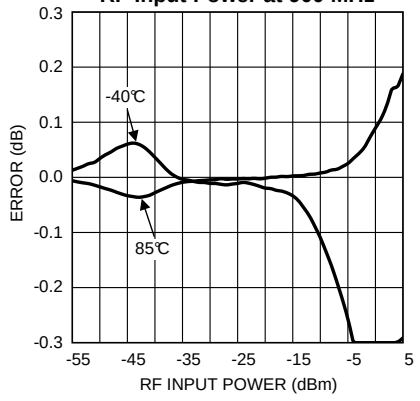


**Figure 40.**

## Typical Performance Characteristics (continued)

Unless otherwise specified, $V_{DD}$ = 2.7V, $T_A$ = 25°C, measured on a limited number of samples.

**Error for 1 dB Input Power Step vs. RF Input Power at 1855 MHz**

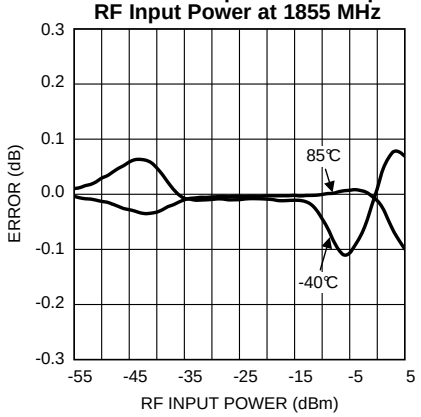


**Figure 41.**

**Error for 1 dB Input Power Step vs. RF Input Power at 2500 MHz**

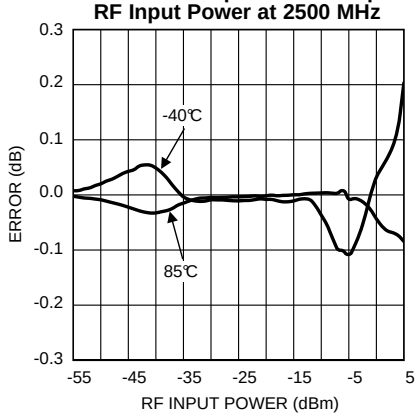


**Figure 42.**

**Error for 1 dB Input Power Step vs. RF Input Power at 3000 MHz**

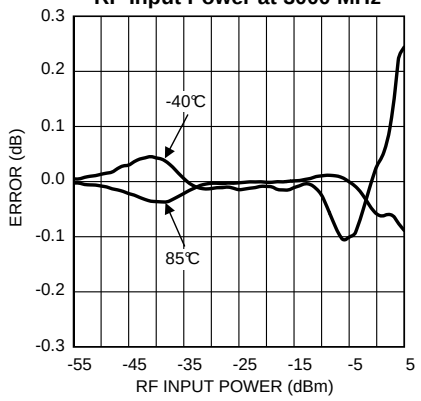


**Figure 43.**

**Error for 1 dB Input Power Step vs. RF Input Power at 3500 MHz**

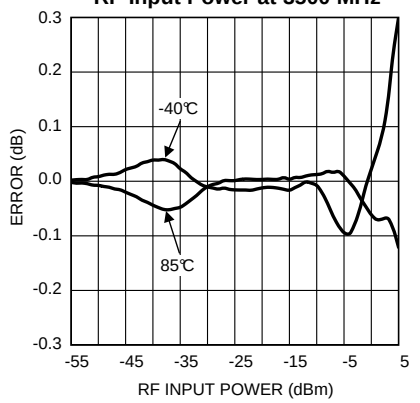


**Figure 44.**

**Error for 1 dB Input Power step vs. RF Input Power at 4000 MHz**

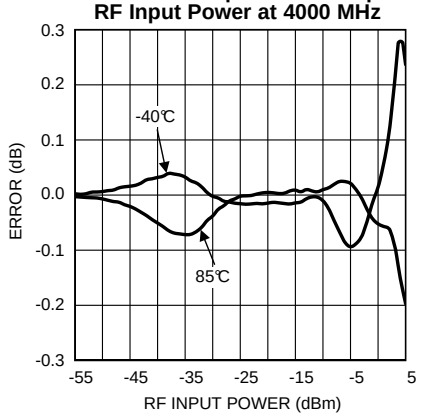


**Figure 45.**

**Error for 10 dB Input Power Step vs. RF Input Power at 50 MHz**

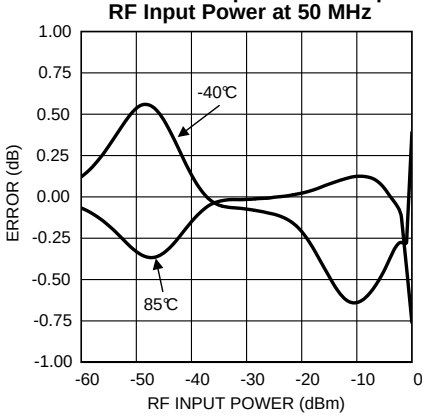


**Figure 46.**

## Typical Performance Characteristics (continued)

Unless otherwise specified, $V_{DD}$ = 2.7V, $T_A$ = 25°C, measured on a limited number of samples.

**Error for 10 dB Input Power Step vs. RF Input Power at 900 MHz**

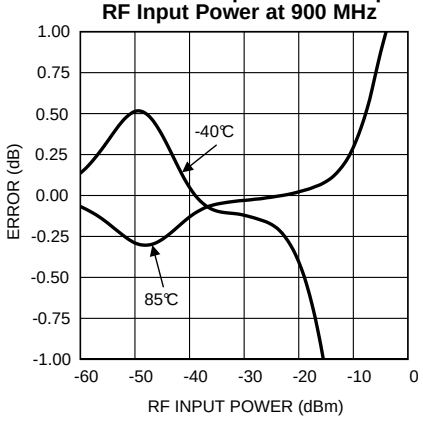


**Figure 47.**

**Error for 10 dB Input Power Step vs. RF Input Power at 1855 MHz**

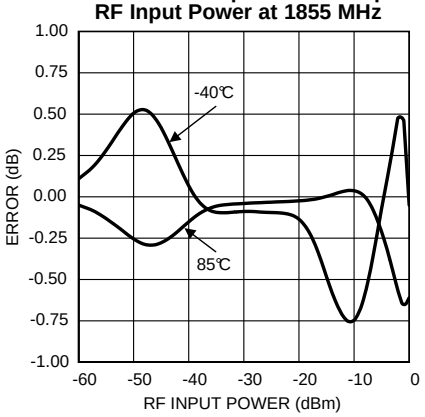


**Figure 48.**

**Error for 10 dB Input Power Step vs. RF Input Power at 2500 MHz**

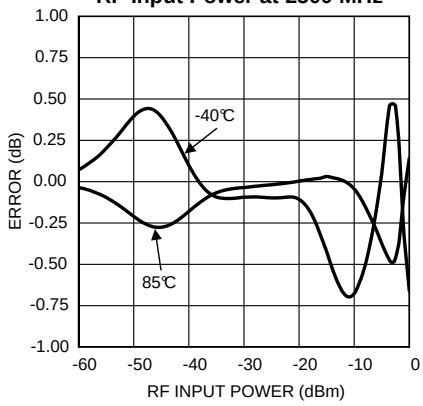


**Figure 49.**

**Error for 10 dB Input Power Step vs. RF Input Power at 3000 MHz**

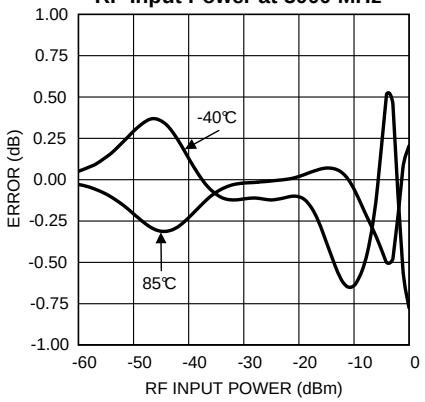


**Figure 50.**

**Error for 10 dB Input Power Step vs. RF Input Power at 3500 MHz**

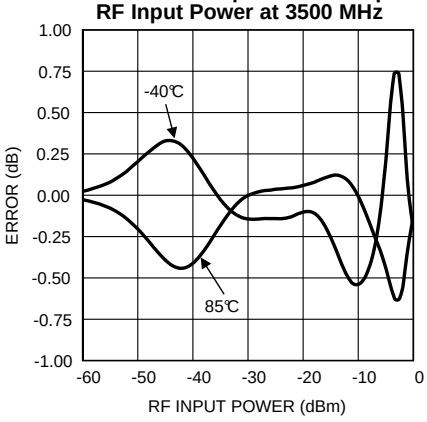


**Figure 51.**

**Error for 10 dB Input Power step vs. RF Input Power at 4000 MHz**

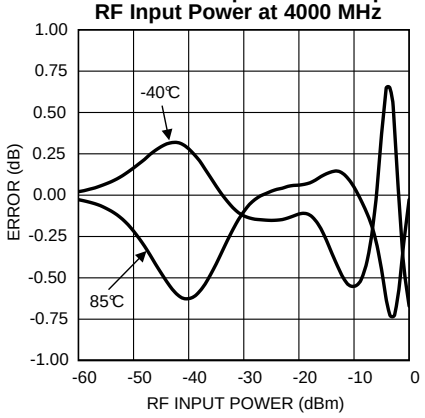


**Figure 52.**

## Typical Performance Characteristics (continued)

Unless otherwise specified, $V_{DD}$ = 2.7V, $T_A$ = 25°C, measured on a limited number of samples.

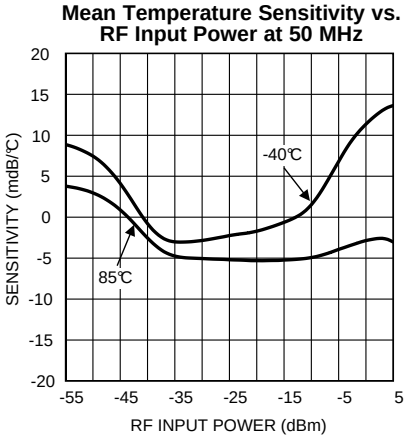


**Figure 53.**

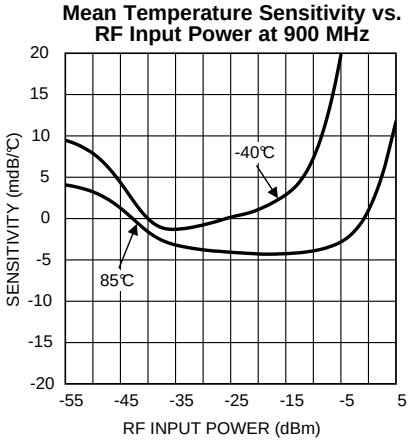


**Figure 54.**

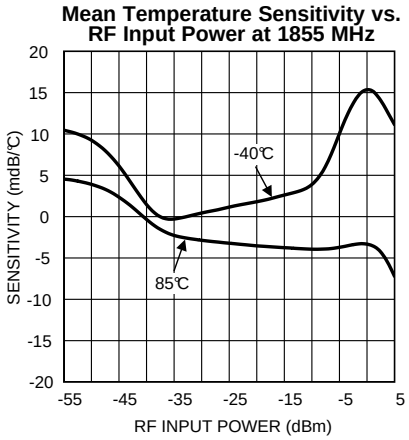


**Figure 55.**

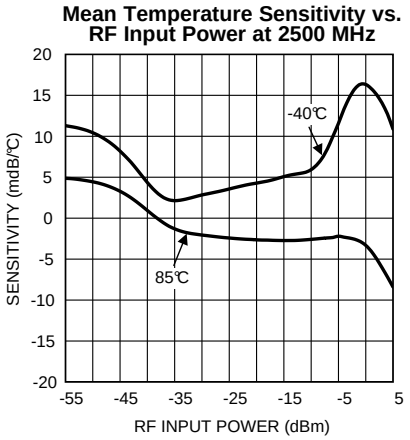


**Figure 56.**

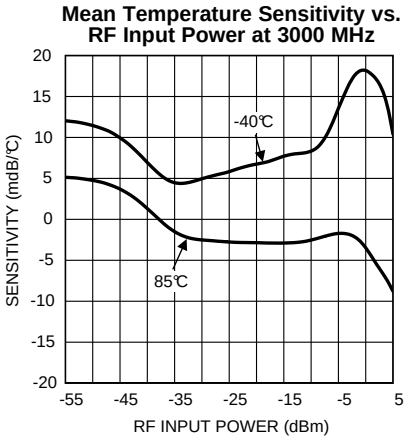


**Figure 57.**

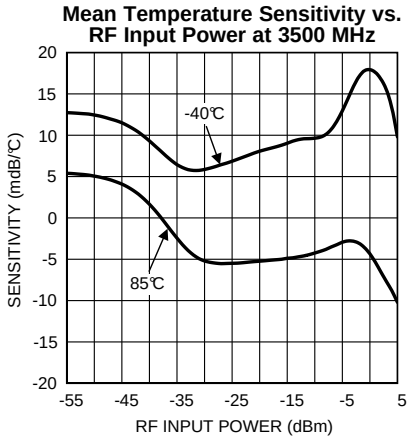


**Figure 58.**

## Typical Performance Characteristics (continued)

Unless otherwise specified, $V_{DD}$ = 2.7V, $T_A$ = 25°C, measured on a limited number of samples.

**Mean Temperature Sensitivity vs. RF Input power at 4000 MHz**

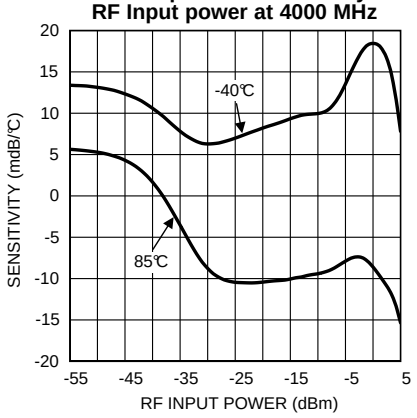


**Figure 59.**

**Temperature Sensitivity (Mean ±3 sigma) vs. RF Input Power at 50 MHz**

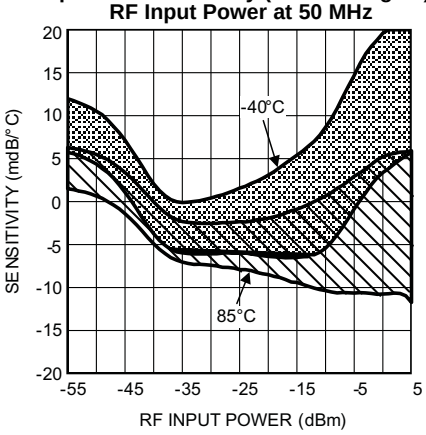


**Figure 60.**

**Temperature Sensitivity (Mean ±3 sigma) vs. RF Input Power at 900 MHz**

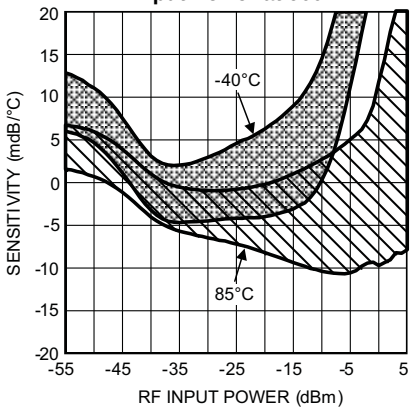


**Figure 61.**

**Temperature Sensitivity (Mean ±3 sigma) vs. RF Input Power at 1855 MHz**

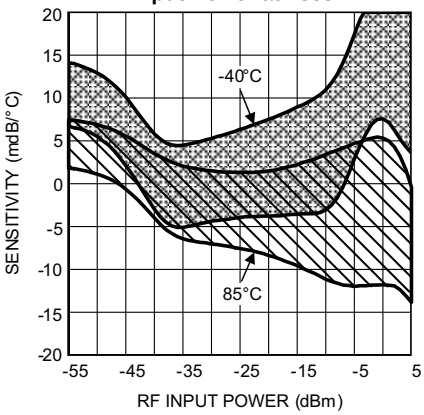


**Figure 62.**

**Temperature Sensitivity (Mean ±3 sigma) vs. RF Input Power at 2500 MHz**

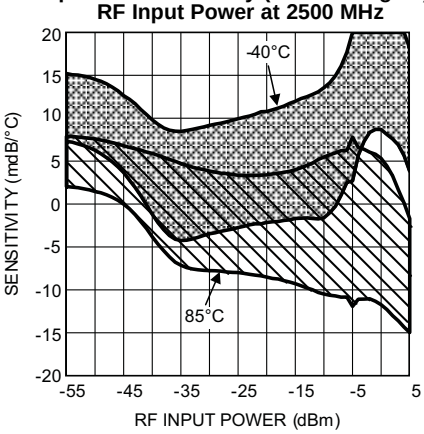


**Figure 63.**

**Temperature Sensitivity (Mean ±3 sigma) vs. RF Input Power at 3000 MHz**

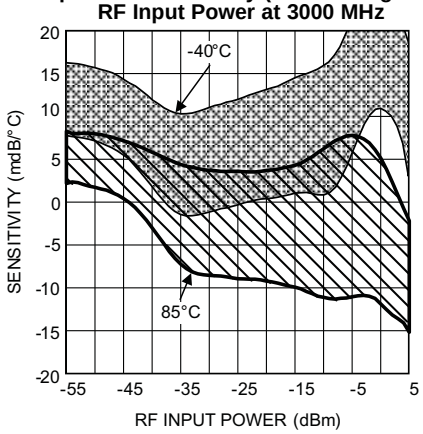


**Figure 64.**

## Typical Performance Characteristics (continued)

Unless otherwise specified, $V_{DD}$ = 2.7V, $T_A$ = 25°C, measured on a limited number of samples.

**Temperature Sensitivity (Mean ±3 sigma) vs. RF Input Power at 3500 MHz**

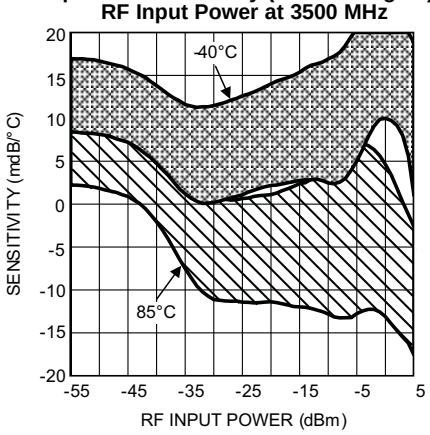


**Figure 65.**

**Temperature Sensitivity (mean ±3 sigma) vs. RF Input Power at 4000 MHz**

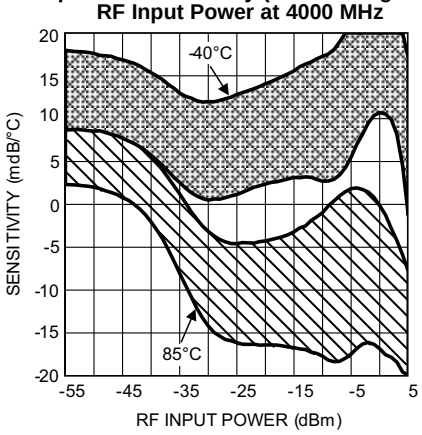


**Figure 66.**

**Output Voltage and Log Conformance Error vs. RF Input Power for Various Modulation Types at 900 MHz**

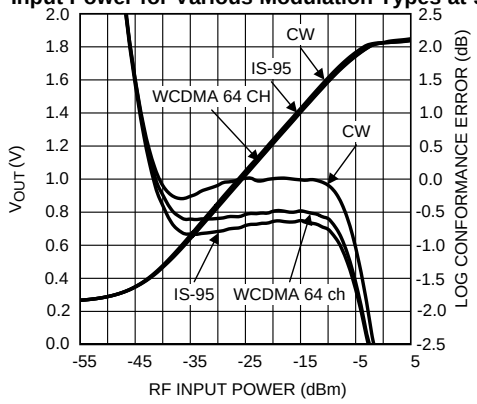


**Figure 67.**

**Output Voltage and Log Conformance Error vs. RF Input Power for Various Modulation Types at 1855 MHz**

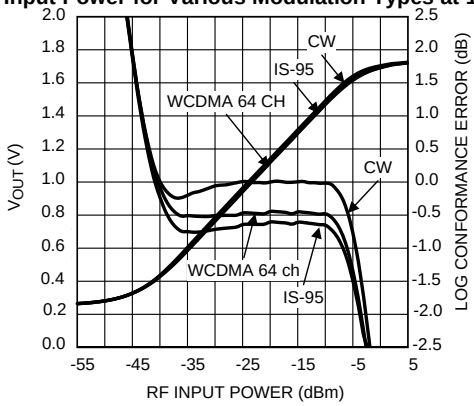


**Figure 68.**

**RF Input Impedance vs. Frequency (Resistance & Reactance)**

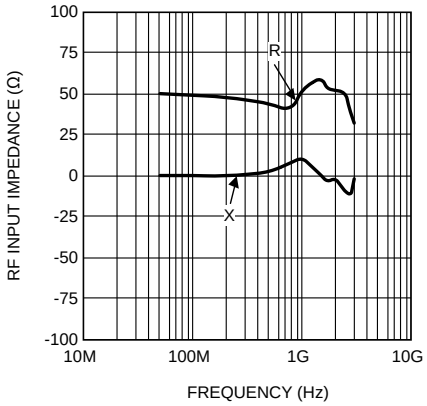


**Figure 69.**

**Output Noise Spectrum vs. Frequency**

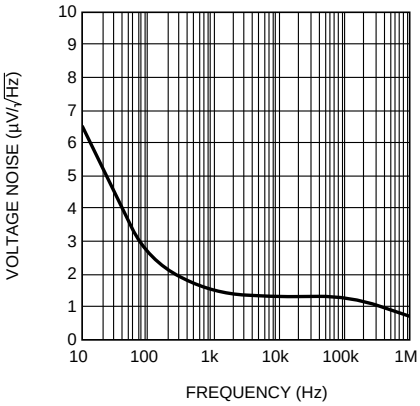


**Figure 70.**

## Typical Performance Characteristics (continued)

Unless otherwise specified, $V_{DD}$ = 2.7V, $T_A$ = 25°C, measured on a limited number of samples.

**Power Supply Rejection Ratio vs. Frequency**

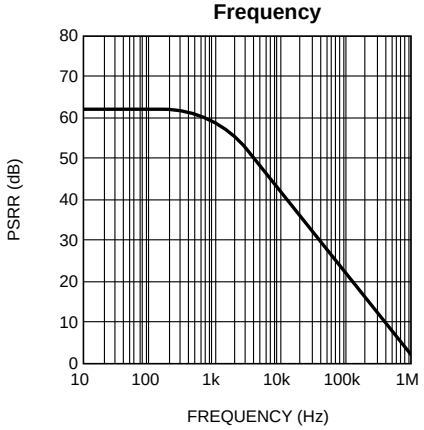


**Figure 71.**

**Output Amplifier Gain & Phase vs. Frequency**

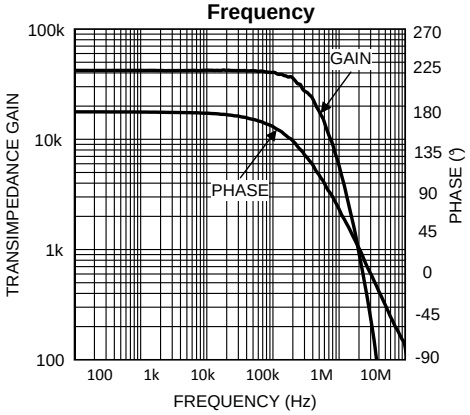


**Figure 72.**

**Sourcing Output Current vs. Output Voltage**

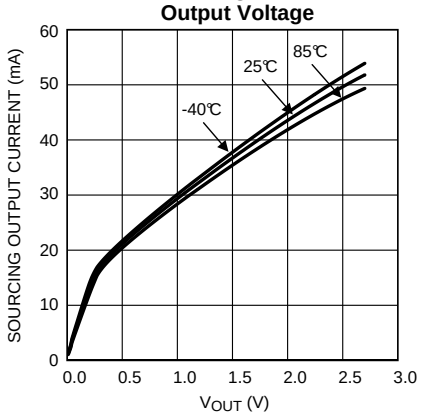


**Figure 73.**

**Sinking Output Current vs. Output Voltage**

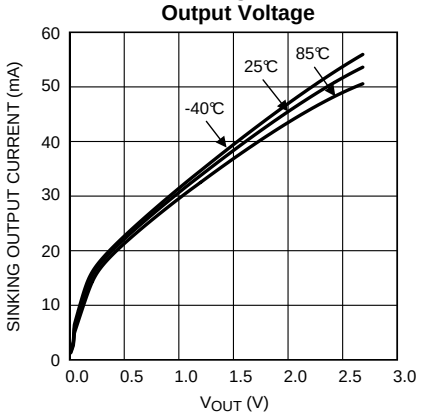


**Figure 74.**

**Output Voltage vs. Sourcing Current**

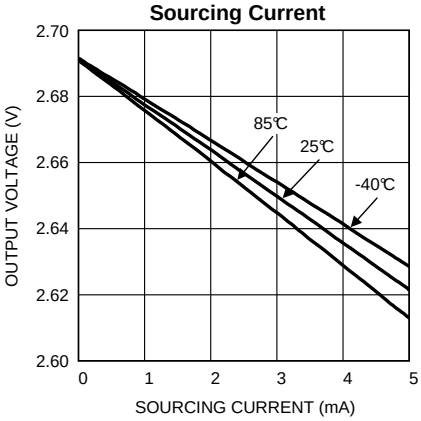


**Figure 75.**

**Output Voltage vs. Sinking Current**

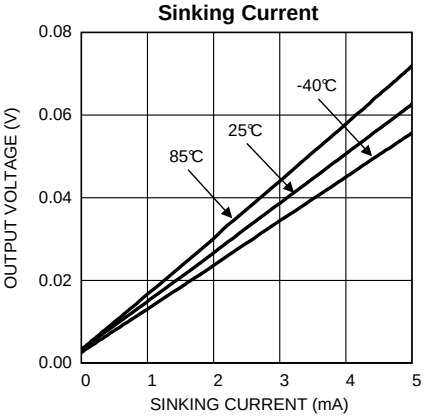


**Figure 76.**

## APPLICATION INFORMATION

The LMH2100 is a versatile logarithmic RF power detector suitable for use in power measurement systems. The LMH2100 is particularly well suited for CDMA and UMTS applications. It produces a DC voltage that is a measure for the applied RF power.

This application section describes the behavior of the LMH2100 and explains how accurate measurements can be performed. Besides this an overview is given of the interfacing options with the connected circuitry as well as the recommended layout for the LMH2100.

### Functionality and Application of RF Power Detectors

This first section describes the functional behavior of RF power detectors and their typical application. Based on a number of key electrical characteristics of RF power detectors, Functionality of RF Power Detectors discusses the functionality of RF power detectors in general and of the LMH2100 LOG detector in particular. Subsequently, Applications of RF Power Detectors describes two important applications of the LMH2100 detector.

#### Functionality of RF Power Detectors

An RF power detector is a device that produces a DC output voltage in response to the RF power level of the signal applied to its input. A wide variety of power detectors can be distinguished, each having certain properties that suit a particular application. This section provides an overview of the key characteristics of power detectors, and discusses the most important types of power detectors. The functional behavior of the LMH2100 is discussed in detail.

##### *Key Characteristics of RF Power Detectors.*

Power detectors are used to accurately measure the power of a signal inside the application. The attainable accuracy of the measurement is therefore dependent upon the accuracy and predictability of the detector transfer function from the RF input power to the DC output voltage.

Certain key characteristics determine the accuracy of RF detectors and they are classified accordingly:

- Temperature Stability
- Dynamic Range
- Waveform Dependency
- Transfer Shape

Each of these aspects is discussed in further detail.

Generally, the transfer function of RF power detectors is slightly temperature dependent. This temperature drift reduces the accuracy of the power measurement, because most applications are calibrated at room temperature. In such systems, the temperature drift significantly contributes to the overall system power measurement error. The temperature stability of the transfer function differs for the various types of power detectors. Generally, power detectors that contain only one or few semiconductor devices (diodes, transistors) operating at RF frequencies attain the best temperature stability.

The dynamic range of a power detector is the input power range for which it creates an accurately reproducible output signal. What is considered accurate is determined by the applied criterion for the detector accuracy; the detector dynamic range is thus always associated with certain power measurement accuracy. This accuracy is usually expressed as the deviation of its transfer function from a certain predefined relationship, such as ”linear in dB" for LOG detectors and ”square-law" transfer (from input RF voltage to DC output voltage) for Mean-Square detectors. For LOG-detectors, the dynamic range is often specified as the power range for which its transfer function follows the ideal linear-in-dB relationship with an error smaller than or equal to ±1 dB. Again, the attainable dynamic range differs considerably for the various types of power detectors.

According to its definition, the average power is a metric for the average energy content of a signal and is not directly a function of the shape of the signal in time. In other words, the power contained in a 0 dBm sine wave is identical to the power contained in a 0 dBm square wave or a 0 dBm WCDMA signal; all these signals have the same average power. Depending on the internal detection mechanism, though, power detectors may produce a slightly different output signal in response to the aforementioned waveforms, even though their average power

level is the same. This is due to the fact that not all power detectors strictly implement the definition formula for signal power, being the mean of the square of the signal. Most types of detectors perform some mixture of peak detection and average power detection. A waveform independent detector response is often desired in applications that exhibit a large variety of waveforms, such that separate calibration for each waveform becomes impractical.

The shape of the detector transfer function from the RF input power to the DC output voltage determines the required resolution of the ADC connected to it. The overall power measurement error is the combination of the error introduced by the detector, and the quantization error contributed by the ADC. The impact of the quantization error on the overall transfer's accuracy is highly dependent on the detector transfer shape, as illustrated in Figure 77 and Figure 78.

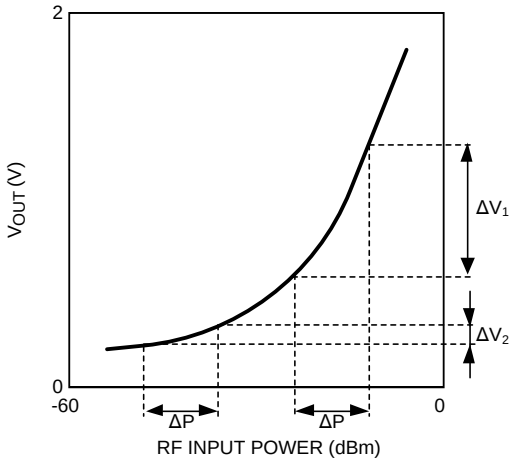


**Figure 77. Convex Detector Transfer Function**

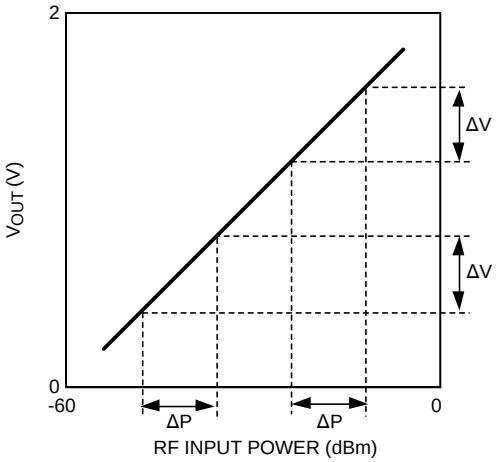


**Figure 78. Linear Transfer Function**

Figure 77 and Figure 78 shows two different representations of the detector transfer function. In both graphs the input power along the horizontal axis is displayed in dBm, since most applications specify power accuracy requirements in dBm (or dB). The figure on the left shows a convex detector transfer function, while the transfer function on the right hand side is linear (in dB). The slope of the detector transfer function — i.e. the detector conversion gain – is of key importance for the impact of the quantization error on the total measurement error. If the detector transfer function slope is low, a change, ΔP, in the input power results only in a small change of the detector output voltage, such that the quantization error will be relatively large. On the other hand, if the detector transfer function slope is high, the output voltage change for the same input power change will be large, such that the quantization error is small. The transfer function on the left has a very low slope at low input power levels, resulting in a relatively large quantization error. Therefore, to achieve accurate power measurement in this region, a high-resolution ADC is required. On the other hand, for high input power levels the quantization error will be very small due to the steep slope of the curve in this region. For accurate power measurement in this region, a much lower ADC resolution is sufficient. The curve on the right has a constant slope over the power range of interest, such that the required ADC resolution for a certain measurement accuracy is constant. For this reason, the LOG-linear curve on the right will generally lead to the lowest ADC resolution requirements for certain power measurement accuracy.

### *Types of RF Power Detectors*

Three different detector types are distinguished based on the four characteristics previously discussed:

- Diode Detector
- (Root) Mean Square Detector
- Logarithmic Detectors

These three types of detectors are discussed in the following sections. Advantages and disadvantages will be presented for each type.

### Diode Detector

A diode is one of the simplest types of RF detectors. As depicted in Figure 79, the diode converts the RF input voltage into a rectified current. This unidirectional current charges the capacitor. The RC time constant of the resistor and the capacitor determines the amount of filtering applied to the rectified (detected) signal.

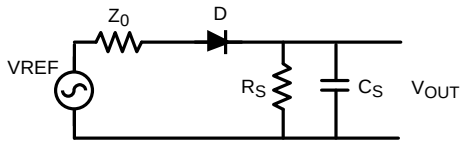


**Figure 79. Diode Detector**

The advantages and disadvantages can be summarized as follows:

- The *temperature stability* of the diode detectors is generally very good, since they contain only one semiconductor device that operates at RF frequencies.
- The *dynamic range* of diode detectors is poor. The conversion gain from the RF input power to the output voltage quickly drops to very low levels when the input power decreases. Typically a dynamic range of 20 – 25 dB can be realized with this type of detector.
- The response of diode detectors is *waveform dependent*. As a consequence of this dependency for example its output voltage for a 0 dBm WCDMA signal is different than for a 0 dBm unmodulated carrier. This is due to the fact that the diode measures peak power instead of average power. The relation between peak power and average power is dependent on the wave shape.
- The *transfer shape* of diode detectors puts high requirements on the resolution of the ADC that reads their output voltage. Especially at low input power levels a very high ADC resolution is required to achieve sufficient power measurement accuracy (See Figure 77).

### (Root) Mean Square Detector

This type of detector is particularly suited for the power measurements of RF modulated signals that exhibits large peak to average power ratio variations. This is because its operation is based on direct determination of the average power and not – like the diode detector – of the peak power.

The advantages and disadvantages can be summarized as follows:

- The *temperature stability* of (R)MS detectors is almost as good as the temperature stability of the diode detector; only a small part of the circuit operates at RF frequencies, while the rest of the circuit operates at low frequencies.
- The *dynamic range* of (R)MS detectors is limited. The lower end of the dynamic range is limited by internal device offsets.
- The response of (R)MS detectors is highly *waveform independent*. This is a key advantage compared to other types of detectors in applications that employ signals with high peak-to-average power variations. For example, the (R)MS detector response to a 0 dBm WCDMA signal and a 0 dBm unmodulated carrier is essentially equal.
- The *transfer shape* of R(MS) detectors has many similarities with the diode detector and is therefore subject to similar disadvantages with respect to the ADC resolution requirements (See Figure 78).

### Logarithmic Detectors

The transfer function of a logarithmic detector has a linear in dB response, which means that the output voltage changes linearly with the RF power in dBm. This is convenient since most communication standards specify transmit power levels in dBm as well.

The advantages and disadvantages can be summarized as follows:

- The *temperature stability* of the LOG detector transfer function is generally not as good as the stability of diode and R(MS) detectors. This is because a significant part of the circuit operates at RF frequencies.
- The *dynamic range* of LOG detectors is usually much larger than that of other types of detectors.
- Since LOG detectors perform a kind of peak detection their response is *wave form dependent*, similar to diode detectors.
- The *transfer shape* of LOG detectors puts the lowest possible requirements on the ADC resolution (See

Figure 78).

### *Characteristics of the LMH2100*

The LMH2100 is a logarithmic RF power detector with approximately 40 dB dynamic range. This dynamic range plus its logarithmic behavior make the LMH2100 ideal for various applications such as wireless transmit power control for CDMA and UMTS applications. The frequency range of the LMH2100 is from 50 MHz to 4 GHz, which makes it suitable for various applications.

The LMH2100 transfer function is accurately temperature compensated. This makes the measurement accurate for a wide temperature range. Furthermore, the LMH2100 can easily be connected to a directional coupler because of its 50Ω input termination. The output range is adjustable to fit the ADC input range. The detector can be switched into a power saving shutdown mode for use in pulsed conditions.

## Applications of RF Power Detectors

RF power detectors can be used in a wide variety of applications. This section discusses two applications. The first example shows the LMH2100 in a Transmit Power Control Loop, the second application measures the Voltage Standing Wave Ratio Measurement.

### *Transmit Power Control Loop*

The key benefit of a transmit power control loop circuit is that it makes the transmit power insensitive to changes in the Power Amplifier (PA) gain control function, such as changes due to temperature drift. When a control loop is used, the transfer function of the PA is eliminated from the overall transfer function. Instead, the overall transfer function is determined by the power detector. The overall transfer function accuracy depends thus on the RF detector accuracy. The LMH2100 is especially suited for this application, due to the accurate temperature stability of its transfer function.

Figure 80 shows a block diagram of a typical transmit power control system. The output power of the PA is measured by the LMH2100 through a directional coupler. The measured output voltage of the LMH2100 is filtered and subsequently digitized by the ADC inside the baseband chip. The baseband adjusts the PA output power level by changing the gain control signal of the RF VGA accordingly. With an input impedance of 50Ω, the LMH2100 can be directly connected to a 30 dB directional coupler without the need for an additional external attenuator. The setup can be adjusted to various PA output ranges by selection of a directional coupler with the appropriate coupling factor.

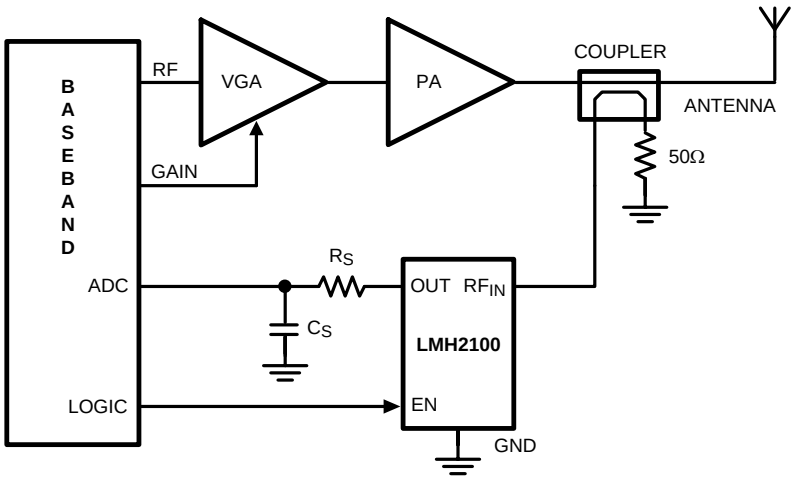


**Figure 80. Transmit Power Control System**

### *Voltage Standing Wave Ratio Measurement*

Transmission in RF systems requires matched termination by the proper characteristic impedance at the transmitter and receiver side of the link. In wireless transmission systems though, matched termination of the antenna can rarely be achieved. The part of the transmitted power that is reflected at the antenna bounces back toward the PA and may cause standing waves in the transmission line between the PA and the antenna. These standing waves can attain unacceptable levels that may damage the PA. A Voltage Standing Wave Ratio (VSWR) measurement is used to detect such an occasion. It acts as an alarm function to prevent damage to the transmitter.

VSWR is defined as the ratio of the maximum voltage divided by the minimum voltage at a certain point on the transmission line:

$$VSWR = \frac{1 + |\Gamma|}{1 - |\Gamma|} \quad (1)$$

Where $\Gamma = V_{REFLECTED} / V_{FORWARD}$ denotes the reflection coefficient.

This means that to determine the VSWR, both the forward (transmitted) and the reflected power levels have to be measured. This can be accomplished by using two LMH2100 RF power detectors according to Figure 81. A directional coupler is used to separate the forward and reflected power waves on the transmission line between the PA and the antenna. One secondary output of the coupler provides a signal proportional to the forward power wave, the other secondary output provides a signal proportional to the reflected power wave. The outputs of both RF detectors that measure these signals are connected to a micro-controller or baseband that calculates the VSWR from the detector output signals.

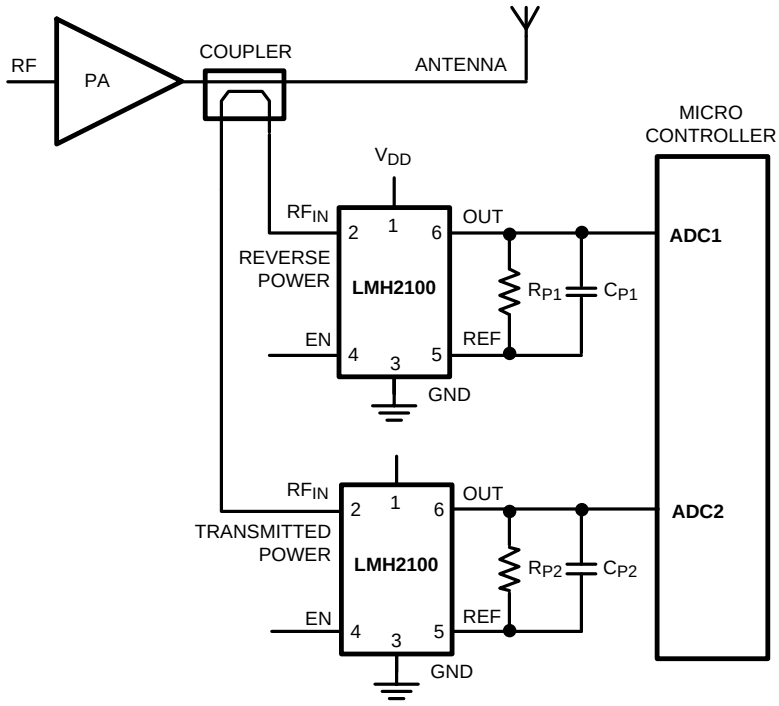


**Figure 81. VSWR Application**

## Accurate Power Measurement

The power measurement accuracy achieved with a power detector is not only determined by the accuracy of the detector itself, but also by the way it is integrated into the application. In many applications some form of calibration is employed to improve the accuracy of the overall system beyond the intrinsic accuracy provided by the power detector. For example, for LOG-detectors calibration can be used to eliminate part to part spread of the LOG-slope and LOG-intercept from the overall power measurement system, thereby improving its power measurement accuracy.

This section shows how calibration techniques can be used to improve the accuracy of a power measurement system beyond the intrinsic accuracy of the power detector itself. The main focus of the section is on power measurement systems using LOG-detectors, specifically the LMH2100, but the more generic concepts can also be applied to other power detectors. Other factors influencing the power measurement accuracy, such as the resolution of the ADC reading the detector output signal will not be considered here since they are not fundamentally due to the power detector.

### Concept of Power Measurements

Power measurement systems generally consists of two clearly distinguishable parts with different functions:

1. A power detector device, that generates a DC output signal (voltage) in response to the power level of the (RF) signal applied to its input.
2. An "estimator" that converts the measured detector output signal into a (digital) numeric value representing the power level of the signal at the detector input.

A sketch of this conceptual configuration is depicted in Figure 82 .

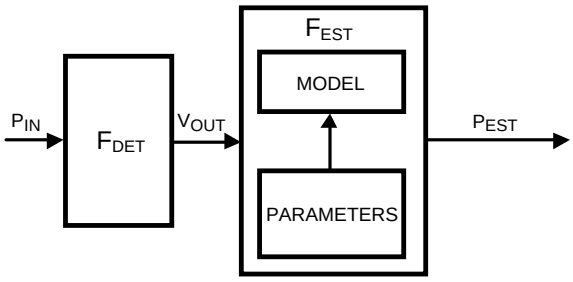


**Figure 82. Generic Concept of a Power Measurement System**

The core of the estimator is usually implemented as a software algorithm, receiving a digitized version of the detector output voltage. Its transfer $F_{EST}$ from detector output voltage to a numerical output should be equal to the inverse of the detector transfer $F_{DET}$ from (RF) input power to DC output voltage. If the power measurement system is ideal, i.e. if no errors are introduced into the measurement result by the detector or the estimator, the measured power $P_{EST}$ - the output of the estimator - and the actual input power $P_{IN}$ should be identical. In that case, the measurement error E, the difference between the two, should be identically zero:

$$\begin{aligned} & E = P_{EST} - P_{IN} \equiv 0 \\ \Leftrightarrow\ & P_{EST} = F_{EST}[F_{DET}(P_{IN})] = P_{IN} \\ \Leftrightarrow\ & F_{EST}(V_{OUT}) = F_{DET}^{-1}(V_{OUT}) \end{aligned} \tag{2}$$

From the expression above it follows that one would design the $F_{EST}$ transfer function to be the inverse of the $F_{DET}$ transfer function.

In practice the power measurement error will not be zero, due to the following effects:

- The detector transfer function is subject to various kinds of random errors that result in uncertainty in the detector output voltage; the detector transfer function is not exactly known.
- The detector transfer function might be too complicated to be implemented in a practical estimator.

The function of the estimator is then to *estimate* the input power $P_{IN}$, i.e. to produce an output $P_{EST}$ such that the power measurement error is - on average - minimized, based on the following information:

1. Measurement of the not completely accurate detector output voltage $V_{OUT}$
2. Knowledge about the detector transfer function $F_{DET}$, for example the shape of the transfer function, the types of errors present (part-to-part spread, temperature drift) etc.

Obviously the total measurement accuracy can be optimized by minimizing the uncertainty in the detector output signal (i.e. select an accurate power detector), and by incorporating as much accurate information about the detector transfer function into the estimator as possible.

The knowledge about the detector transfer function is condensed into a mathematical model for the detector transfer function, consisting of:

- A formula for the detector transfer function.
- Values for the parameters in this formula.

The values for the parameters in the model can be obtained in various ways. They can be based on measurements of the detector transfer function in a precisely controlled environment (parameter extraction). If the parameter values are separately determined for each individual device, errors like part-to-part spread are eliminated from the measurement system.

Obviously, errors may occur when the operating conditions of the detector (e.g. the temperature) become significantly different from the operating conditions during calibration (e.g. room temperature). Subsequent sections will discuss examples of simple estimators for power measurements that result in a number of commonly used metrics for the power measurement error: the LOG-Conformance Error, the Temperature Drift Error, the Temperature Sensitivity and Temperature Drift Error.

### LOG-Conformance Error

Probably the simplest power measurement system that can be realized is obtained when the LOG-detector transfer function is modelled as a perfect linear-in-dB relationship between the input power and output voltage:

$$V_{OUT,MOD} = F_{DET,MOD}(P_{IN}) = K_{SLOPE}(P_{IN} - P_{INTERCEPT}) \tag{3}$$

in which $K_{SLOPE}$ represents the LOG-slope and $P_{INTERCEPT}$ the LOG-intercept. The estimator based on this model implements the inverse of the model equation, i.e.

$$P_{EST} = F_{EST}(V_{OUT}) = \frac{V_{OUT}}{K_{SLOPE}} + P_{INTERCEPT} \tag{4}$$

The resulting power measurement error, the LOG-conformance error, is thus equal to:

$$E_{LCE} = P_{EST} - P_{IN} = \frac{V_{OUT}}{K_{SLOPE}} - (P_{IN} - P_{INTERCEPT}) = \frac{V_{OUT} - V_{OUT,MOD}}{K_{SLOPE}} \tag{5}$$

The most important contributions to the LOG-conformance error are generally:

- The deviation of the actual detector transfer function from an ideal Logarithm (the transfer function is nonlinear in dB).
- Drift of the detector transfer function over various environmental conditions, most importantly temperature; $K_{SLOPE}$ and $P_{INTERCEPT}$ are usually determined for room temperature only.
- Part-to-part spread of the (room temperature) transfer function.

The latter component is conveniently removed by means of calibration, i.e. if the LOG slope and LOG-intercept are determined for each individual detector device (at room temperature). This can be achieved by measurement of the detector output voltage - at room temperature - for a series of different power levels in the LOG-linear range of the detector transfer function. The slope and intercept can then be determined by means of linear regression.

An example of this type of error and its relationship to the detector transfer function is depicted in Figure 83.

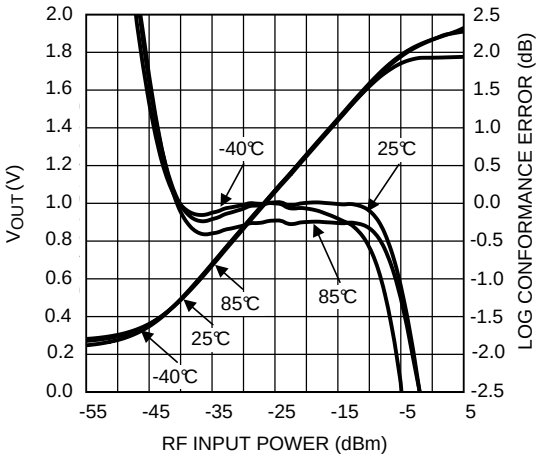


**Figure 83. LOG-Conformance Error and LOG-Detector Transfer Function**

In the center of the detector's dynamic range, the LOG-conformance error is small, especially at room temperature; in this region the transfer function closely follows the linear-in-dB relationship while $K_{SLOPE}$ and $P_{INTERCEPT}$ are determined based on room temperature measurements. At the temperature extremes the error in the center of the range is slightly larger due to the temperature drift of the detector transfer function. The error rapidly increases toward the top and bottom end of the detector's dynamic range; here the detector saturates and its transfer function starts to deviate significantly from the ideal LOG-linear model. The detector dynamic range is usually defined as the power range for which the LOG conformance error is smaller than a specified amount. Often an error of ±1 dB is used as a criterion.

### Temperature Drift Error

A more accurate power measurement system can be obtained if the first error contribution, due to the deviation from the ideal LOG-linear model, is eliminated. This is achieved if the actual measured detector transfer function at room temperature is used as a model for the detector, instead of the ideal LOG-linear transfer function used in the previous section.

The formula used for such a detector is:

$V_{OUT,MOD} = F_{DET}(P_{IN}, T_O)$

where $T_O$ represents the temperature during calibration (room temperature). The transfer function of the corresponding estimator is thus the inverse of this:

$$P_{EST} = F_{DET}^{-1}[V_{OUT(T)}, T_0] \tag{6}$$

In this expression $V_{OUT}(T)$ represents the measured detector output voltage at the operating temperature T.

The resulting measurement error is only due to drift of the detector transfer function over temperature, and can be expressed as:

$$\begin{aligned} E_{DRIFT}(T,T_0) &= P_{EST} - P_{IN} = F_{DET}^{-1}[V_{OUT(T)}, T_0] - P_{IN} \\ &= F_{DET}^{-1}[V_{OUT}(T), T_0] - F_{DET}^{-1}[V_{OUT}(T), T)] \end{aligned} \tag{7}$$

Unfortunately, the (numeric) inverse of the detector transfer function at different temperatures makes this expression rather impractical. However, since the drift error is usually small $V_{OUT}(T)$ is only slightly different from $V_{OUT}(T_O)$. This means that we can apply the following approximation:

$$E_{DRIFT}(T,T_0) \approx E_{DRIFT}(T_0,T_0) + (T - T_0)\frac{\partial}{\partial T}\{F_{DET}^{-1}[V_{OUT}(T),T_0] - F_{DET}^{-1}[V_{OUT}(T),T]\} \quad (8)$$

This expression is easily simplified by taking the following considerations into account:

- The drift error at the calibration temperature $E(T_O,T_O)$ equals zero (by definition).
- The estimator transfer $F_{DET}(V_{OUT},T_O)$ is not a function of temperature; the estimator output changes over temperature only due to the temperature dependence of $V_{OUT}$.
- The actual detector input power $P_{IN}$ is not temperature dependent (in the context of this expression).
- The derivative of the estimator transfer function to $V_{OUT}$ equals approximately $1/K_{SLOPE}$ in the LOG-linear region of the detector transfer function (the region of interest).

Using this, we arrive at:

$$\begin{aligned} E_{DRIFT}(T,T_0) &\approx (T - T_0)\frac{\partial}{\partial T} F_{DET}^{-1}[V_{OUT}(T),T_0] \\ &= (T - T_0)\ \frac{\partial V_{OUT}(T)}{\partial T}\ \frac{\partial}{\partial V_{OUT}} F_{DET}^{-1}[V_{OUT}(T),T_0] \\ &\approx \frac{V_{OUT}(T) - V_{OUT}(T_0)}{K_{SLOPE}} \end{aligned} \quad (9)$$

This expression is very similar to the expression of the LOG-conformance error determined previously. The only difference is that instead of the output of the ideal LOG-linear model, the actual detector output voltage at the calibration temperature is now subtracted from the detector output voltage at the operating temperature.

Figure 84 depicts an example of the drift error.

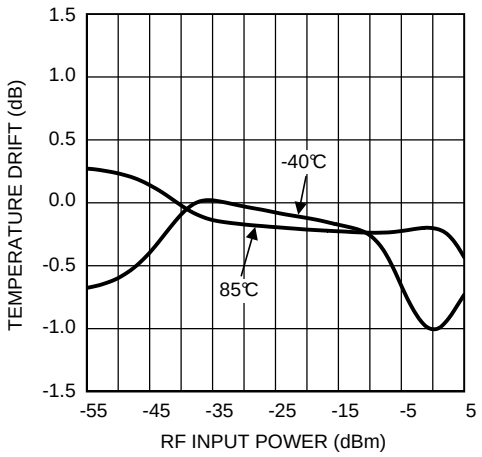


**Figure 84. Temperature Drift Error of the LMH2100 at f = 1855 MHz**

In agreement with the definition, the temperature drift error is zero at the calibration temperature. Further, the main difference with the LOG-conformance error is observed at the top and bottom end of the detection range; instead of a rapid increase the drift error settles to a small value at high and low input power levels due to the fact that the detector saturation levels are relatively temperature independent.

In a practical application it may not be possible to use the exact inverse detector transfer function as the algorithm for the estimator. For example it may require too much memory and/or too much factory calibration time. However, using the ideal LOG-linear model in combination with a few extra data points at the top and bottom end of the detection range - where the deviation is largest - can already significantly reduce the power measurement error.

### *Temperature Compensation*

A further reduction of the power measurement error is possible if the operating temperature is measured in the application. For this purpose, the detector model used by the estimator should be extended to cover the temperature dependency of the detector.

Since the detector transfer function is generally a smooth function of temperature (the output voltage changes gradually over temperature), the temperature is in most cases adequately modeled by a first-order or second-order polynomial, i.e.

$$V_{OUT,MOD} = F_{DET}(P_{IN},T_0)[1 + (T-T_0)TC_1(P_{IN}) + (T-T_0)^2TC_2(P_{IN}) + O(T^3)] \quad (10)$$

The required temperature dependence of the estimator, to compensate for the detector temperature dependence can be approximated similarly:

$$P_{EST} = F_{DET}^{-1}[V_{OUT}(T),T_0]\{1 + (T-T_0)S_1[V_{OUT}(T)] + + (T-T_0)^2S_2[V_{OUT}(T)] + O(T^3)\}$$
$$\approx F_{DET}^{-1}[V_{OUT}(T),T_0]\{1 + (T-T_0)S_1[V_{OUT}(T)]\} \quad (11)$$

The last approximation results from the fact that a first-order temperature compensation is usually sufficiently accurate. The remainder of this section will therefore concentrate on first-order compensation. For second and higher-order compensation a similar approach can be followed.

Ideally, the temperature drift could be completely eliminated if the measurement system is calibrated at various temperatures and input power levels to determine the Temperature Sensitivity $S_1$. In a practical application, however that is usually not possible due to the associated high costs. The alternative is to use the average temperature drift in the estimator, instead of the temperature sensitivity of each device individually. In this way it becomes possible to eliminate the systematic (reproducible) component of the temperature drift without the need for calibration at different temperatures during manufacturing. What remains is the random temperature drift, which differs from device to device. Figure 85 illustrates the idea. The graph at the left schematically represents the behavior of the drift error versus temperature at a certain input power level for a large number of devices.

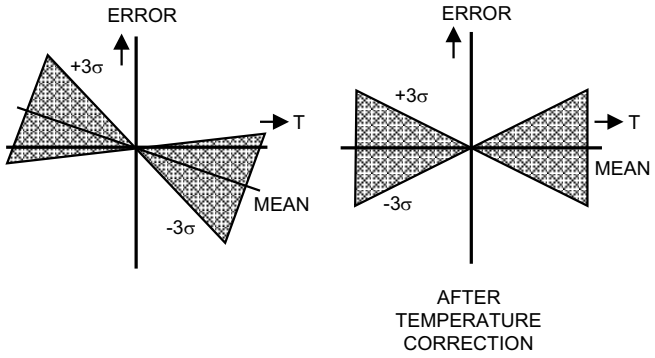


**Figure 85. Elimination of the Systematic Component from the Temperature Drift**

The mean drift error represents the reproducible - systematic - part of the error, while the mean ± 3 sigma limits represent the combined systematic plus random error component. Obviously the drift error must be zero at calibration temperature $T_0$. If the systematic component of the drift error is included in the estimator, the total drift error becomes equal to only the random component, as illustrated in the graph at the right of Figure 85. A significant reduction of the temperature drift error can be achieved in this way only if:

- The systematic component is significantly larger than the random error component (otherwise the difference is negligible).
- The operating temperature is measured with sufficient accuracy.

It is essential for the effectiveness of the temperature compensation to assign the appropriate value to the temperature sensitivity $S_1$. Two different approaches can be followed to determine this parameter:

- Determination of a single value to be used over the entire operating temperature range.
- Division of the operating temperature range in segments and use of separate values for each of the segments.

Also for the first method, the accuracy of the extracted temperature sensitivity increases when the number of measurement temperatures increases. Linear regression to temperature can then be used to determine the two parameters of the linear model for the temperature drift error: the first order temperature sensitivity $S_1$ and the best-fit (room temperature) value for the power estimate at $T_0$: $F_{DET}[V_{OUT}(T),T_0]$. Note that to achieve an overall - over all temperatures - minimum error, the room temperature drift error in the model can be non-zero at the calibration temperature (which is not in agreement with the strict definition).

The second method does not have this drawback but is more complex. In fact, segmentation of the temperature range is a form of higher-order temperature compensation using only a first-order model for the different segments: one for temperatures below 25°C, and one for temperatures above 25°C. The mean (or typical) temperature sensitivity is the value to be used for compensation of the systematic drift error component. Figure 87 shows the temperature drift error without and with temperature compensation using two segments. With compensation the systematic component is completely eliminated; the remaining random error component is centered around zero. Note that the random component is slightly larger at −40°C than at 85°C.

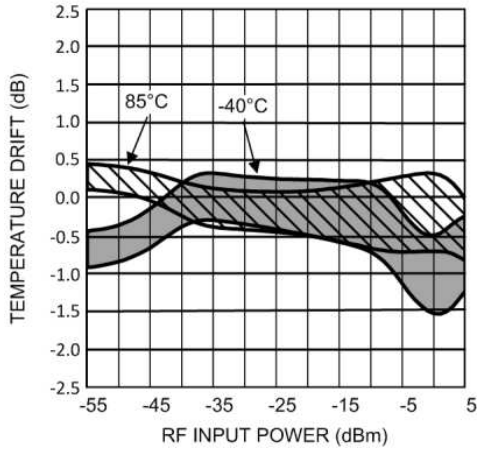


**Figure 86. Temperature Drift Error without Temperature Compensation**

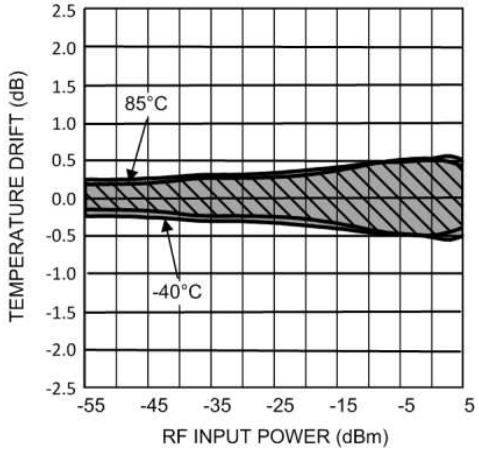


**Figure 87. Temperature Drift Error without with Temperature Compensation**

In a practical power measurement system, temperature compensation is usually only applied to a small power range around the maximum power level for two reasons:

- The various communication standards require the highest accuracy in this range to limit interference.
- The temperature sensitivity itself is a function of the power level it becomes impractical to store a large number of different temperature sensitivity values for different power levels.

The 2.7 V DC and AC Electrical Characteristics in the datasheet specifies the temperature sensitivity for the aforementioned two segments at an input power level of −10 dBm (near the top-end of the detector dynamic range). The typical value represents the mean which is to be used for calibration.

### *Differential Power Errors*

Many third generation communication systems contain a power control loop through the base station and mobile unit that requests both to frequently update the transmit power level by a small amount (typically 1 dB). For such applications it is important that the actual change of the transmit power is sufficiently close to the requested power change.

The error metrics in the datasheet that describe the accuracy of the detector for a change in the input power are $E_{1\ dB}$ (for a 1 dB change in the input power) and $E_{10\ dB}$ (for a 10 dB step, or ten consecutive steps of 1 dB). Since it can be assumed that the temperature does not change during the power step the differential error equals the difference of the drift error at the two involved power levels:

$$E_{1dB(P_{IN},T)} = E_{DRIFT}(P_{IN}+1dB,T) - E_{DRIFT}(P_{IN},T)$$
$$E_{10dB(P_{IN},T)} = E_{DRIFT}(P_{IN}+10dB,T) - E_{DRIFT}(P_{IN},T) \quad (12)$$

It should be noted that the step error increases significantly when one (or both) power levels in the above expression are outside the detector dynamic range. For $E_{10\ dB}$ this occurs when $P_{IN}$ is less than 10 dB below the maximum input power of the dynamic range, $P_{MAX}$.

### Detector Interfacing

For optimal performance of the LMH2100, it is important that all its pins are connected to the surrounding circuitry in the appropriate way. This section discusses guidelines and requirements for the electrical connection of each pin of the LMH2100 to ensure proper operation of the device. Starting from a block diagram, the function of each pin is elaborated. Subsequently, the details of the electrical interfacing are separately discussed for each pin. Special attention will be paid to the output filtering options and the differences between single ended and differential interfacing with an ADC.

### 3.1 Block Diagram of the LMH2100

The block diagram of the LMH2100 is depicted in Figure 88.

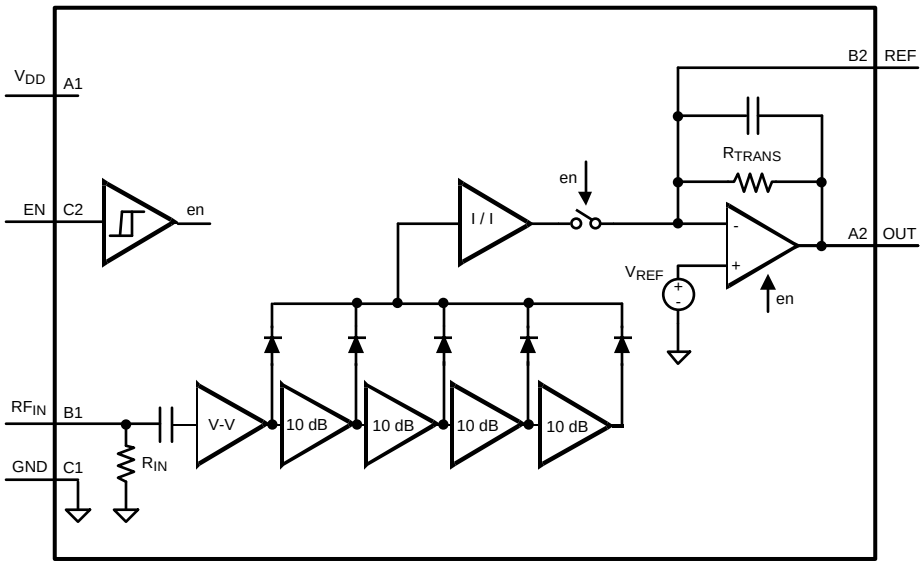


**Figure 88. Block Diagram of the LMH2100**

The core of the LMH2100 is a progressive compression LOG-detector consisting of four gain stages. Each of these saturating stages has a gain of approximately 10 dB and therefore realizes about 10 dB of the detector dynamic range. The five diode cells perform the actual detection and convert the RF signal to a DC current. This DC current is subsequently supplied to the transimpedance amplifier at the output, that converts it into an output voltage. In addition, the amplifier provides buffering of and applies filtering to the detector output signal. To prevent discharge of filtering capacitors between OUT and GND in shutdown, a switch is inserted at the amplifier input that opens in shutdown to realize a high impedance output of the device.

### RF Input

RF parts typically use a characteristic impedance of 50Ω. To comply with this standard the LMH2100 has an input impedance of 50Ω. Using a characteristic impedance other then 50Ω will cause a shift of the logarithmic intercept with respect to the value given in the 2.7 V DC and AC Electrical Characteristics. This intercept shift can be calculated according to the following formula: Equation 13.

$$P_{INT\text{-}SHIFT} = 10\ LOG\left(\frac{2\ R_{SOURCE}}{R_{SOURCE} + 50}\right) \quad (13)$$

The intercept will shift to higher power levels for $R_{SOURCE}$ > 50Ω, and will shift to lower power levels for $R_{SOURCE}$ < 50Ω.

### Shutdown

To save power, the LMH2100 can be brought into a low-power shutdown mode. The device is active for EN = HIGH ($V_{EN}$>1.1V) and in the low-power shutdown mode for EN = LOW ($V_{EN}$ < 0.6V). In this state the output of the LMH2100 is switched to a high impedance mode. Using the shutdown function, care must be taken not to exceed the absolute maximum ratings. Forcing a voltage to the enable input that is 400 mV higher than $V_{DD}$ or 400 mV lower than GND will damage the device and further operations is not ensured. The absolute maximum ratings can also be exceeded when the enable EN is switched to HIGH (from shutdown to active mode) while the supply voltage is low (off). This should be prevented at all times. A possible solution to protect the part is to add a resistor of 100 kΩ in series with the enable input.

### Output and Reference

This section describes the possible filtering techniques that can be applied to reduce ripple in the detector output voltage. In addition two different topologies to connect the LMH2100 to an ADC are elaborated.

### Filtering

The output voltage of the LMH2100 is a measure for the applied RF signal on the RF input pin. Usually, the applied RF signal contains AM modulation that causes low frequency ripple in the detector output voltage. CDMA signals for instance contain a large amount of amplitude variations. Filtering of the output signal can be used to eliminate this ripple. The filtering can either be realized by a low pass output filter or a low pass feedback filter. Those two techniques are depicted in Figure 89 and Figure 90.

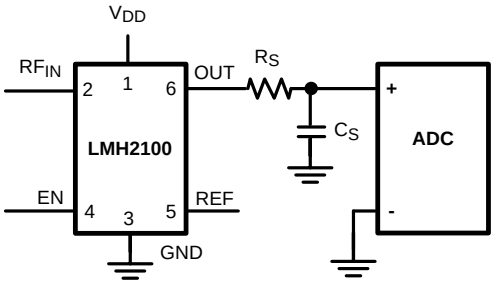


**Figure 89. Low Pass Output Filter**

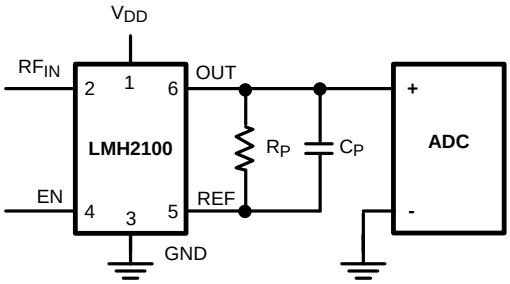


**Figure 90. Low Pass Feedback Filter**

Depending on the system requirements one of the these filtering techniques can be selected. The low pass output filter has the advantage that it preserves the output voltage when the LMH2100 is brought into shutdown. This is elaborated in Output Behavior in Shutdown. In the feedback filter, resistor $R_P$ discharges capacitor $C_P$ in shutdown and therefore changes the output voltage of the device.

A disadvantage of the low pass output filter is that the series resistor $R_S$ limits the output drive capability. This may cause inaccuracies in the voltage read by an ADC when the ADC input impedance is not significantly larger than $R_S$. In that case, the current flowing through the ADC input induces an error voltage across filter resistor $R_S$. The low pass feedback filter doesn't have this disadvantage.

Note that adding an external resistor between OUT and REF reduces the transfer gain (LOG-slope and LOG-intercept) of the device. The internal feedback resistor sets the gain of the transimpedance amplifier.

The filtering of the low pass output filter is realized by resistor $R_S$ and capacitor $C_S$. The −3 dB bandwidth of this filter can then be calculated by: $f_{-3\ dB} = 1 / 2\pi R_S C_S$. The bandwidth of the low pass feedback filter is determined by external resistor $R_P$ in parallel with the internal resistor $R_{TRANS}$, and external capacitor $C_P$ in parallel with internal capacitor $C_{TRANS}$ (see Figure 93). The −3 dB bandwidth of the feedback filter can be calculated by $f_{-3\ dB} = 1 / 2\pi\ (R_P // R_{TRANS})\ (C_P + C_{TRANS})$. The bandwidth set by the internal resistor and capacitor (when no external components are connected between OUT and REF) equals $f_{-3\ dB} = 1 / 2\pi\ R_{TRANS}\ C_{TRANS}$ = 450 kHz.

### Interface to the ADC

The LMH2100 can be connected to the ADC with a single ended or a differential topology. The single ended topology connects the output of the LMH2100 to the input of the ADC and the reference pin is not connected. In a differential topology, both the output and the reference pins of the LMH2100 are connected to the ADC. The topologies are depicted in Figure 91 and Figure 92.

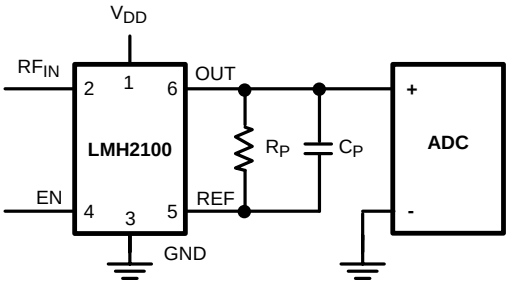


**Figure 91. Single Ended**

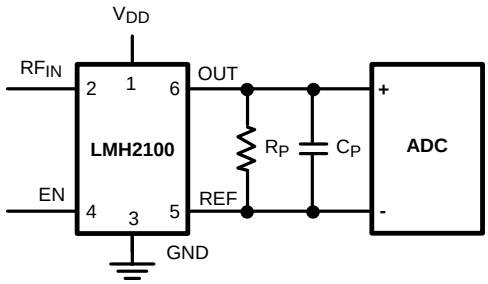


**Figure 92. Differential Application**

The differential topology has the advantage that it is compensated for temperature drift of the internal reference voltage. This can be explained by looking at the transimpedance amplifier of the LMH2100 (Figure 93).

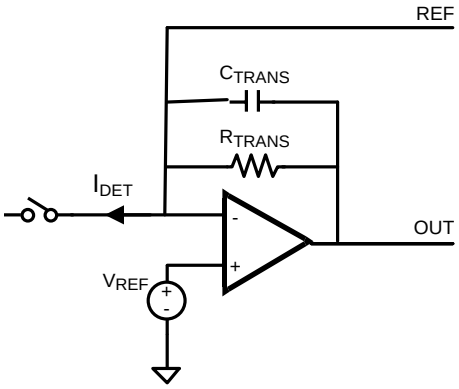


**Figure 93. Output Stage of the LMH2100**

It can be seen that the output of the amplifier is set by the detection current $I_{DET}$ multiplied by the resistor $R_{TRANS}$ plus the reference voltage $V_{REF}$:

$V_{OUT} = I_{DET} R_{TRANS} + V_{REF}$

$I_{DET}$ represents the detector current that is proportional to the RF input power. The equation shows that temperature variations in $V_{REF}$ are also present in the output $V_{OUT}$. In case of a single ended topology the output is the only pin that is connected to the ADC. The ADC voltage for single ended is thus:

Single ended: $V_{ADC} = I_{DET} R_{TRANS} + V_{REF}$

A differential topology also connects the reference pin, which is the value of reference voltage $V_{REF}$. The ADC reads $V_{OUT} - V_{REF}$:

Differential: $V_{ADC} = V_{OUT} - V_{REF} = I_{DET} R_{TRANS}$

The resulting equation doesn't contain the reference voltage $V_{REF}$ anymore. Temperature variations in this reference voltage are therefore not measured by the ADC.

### Output Behavior in Shutdown

In order to save power, the LMH2100 can be used in pulsed mode, such that it is active to perform the power measurement only during a fraction of the time. During the remaining time the device is in low-power shutdown. Applications using this approach usually require that the output value is available at all times, also when the LMH2100 is in shutdown. The settling time in active mode, however, should not become excessively large. This can be realized by the combination of the LMH2100 and a low pass output filter (see Figure 89), as discussed below.

In active mode, the filter capacitor $C_S$ is charged to the output voltage of the LMH2100 — which in this mode has a low output impedance to enable fast settling. During shutdown-mode, the capacitor should preserve this voltage. Discharge of $C_S$ through any current path should therefore be avoided in shutdown. The output impedance of the LMH2100 becomes high in shutdown, such that the discharge current cannot flow from the capacitor top plate, through $R_S$, and the LMH2100's OUT pin to GND. This is realized by the internal shutdown mechanism of the output amplifier and by the switch depicted in Figure 93. Additionally, it should be ensured that the ADC input impedance is high as well, to prevent a possible discharge path through the ADC.

## Board Layout Recommendations

As with any other RF device, careful attention must me paid to the board layout. If the board layout isn't properly designed, unwanted signals can easily be detected or interference will be picked up. This section gives guidelines for proper board layout for the LMH2100.

Electrical signals (voltages/currents) need a finite time to travel through a trace or transmission line. RF voltage levels at the generator side and at the detector side can therefore be different. This is not only true for the RF strip line, but for all traces on the PCB. Signals at different locations or traces on the PCB will be in a different phase of the RF frequency cycle. Phase differences in, e.g. the voltage across neighboring lines, may result in crosstalk between lines, due to parasitic capacitive or inductive coupling. This crosstalk is further enhanced by the fact that all traces on the PCB are susceptible to resonance. The resonance frequency depends on the trace geometry. Traces are particularly sensitive to interference when the length of the trace corresponds to a quarter of the wavelength of the interfering signal or a multiple thereof.

## Supply Lines

Since the PSRR of the LMH2100 is finite, variations of the supply can result in some variation at the output. This can be caused among others by RF injection from other parts of the circuitry or the on/off switching of the PA.

### Positive Supply ($V_{DD}$)

In order to minimize the injection of RF interference into the LMH2100 through the supply lines, the phase difference between the PCB traces connecting to $V_{DD}$ and GND should be minimized. A suitable way to achieve this is to short both connections for RF. This can be done by placing a small decoupling capacitor between the $V_{DD}$ and GND. It should be placed as close as possible to the $V_{DD}$ and GND pins of the LMH2100 as indicated in Figure 94. Be aware that the resonance frequency of the capacitor itself should be above the highest RF frequency used in the application, since the capacitor acts as an inductor above its resonance frequency.

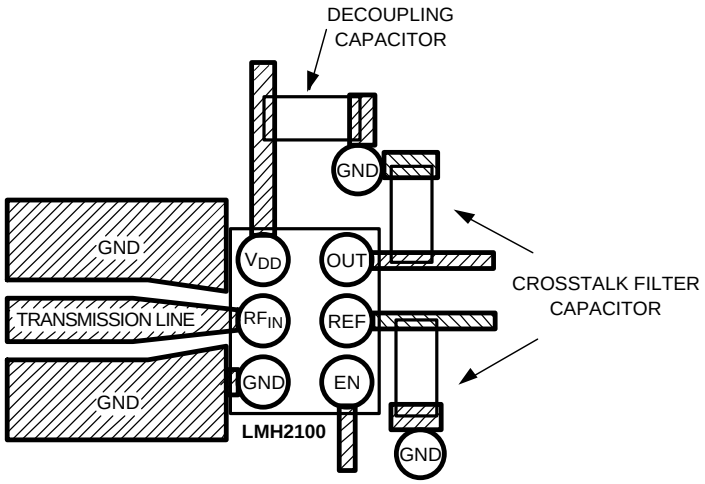


**Figure 94. Recommended Board Layout**

Low frequency supply voltage variations due to PA switching might result in a ripple at the output voltage. The LMH2100 has a Power Supply Rejection Ration of 60 dB for low frequencies.

### Ground (GND)

The LMH2100 needs a ground plane free of noise and other disturbing signals. It is important to separate the RF ground return path from the other grounds. This is due to the fact that the RF input handles large voltage swings. A power level of 0 dBm will cause a voltage swing larger than 0.6 $V_{PP}$, over the internal 50Ω input resistor. This will result in a significant RF return current toward the source. It is therefore recommended that the RF ground return path not be used for other circuits in the design. The RF path should be routed directly back to the source without loops.

## RF Input Interface

The LMH2100 is designed to be used in RF applications, having a characteristic impedance of 50Ω. To achieve this impedance, the input of the LMH2100 needs to be connected via a 50Ω transmission line. Transmission lines can be easily created on PCBs using microstrip or (grounded) coplanar waveguide (GCPW) configurations. This section will discuss both configurations in a general way. For more details about designing microstrip or GCPW transmission lines, a microwave designer handbook is recommended.

## Microstrip Configuration

One way to create a transmission line is to use a microstrip configuration. A cross section of the configuration is shown in Figure 95, assuming a two layer PCB.

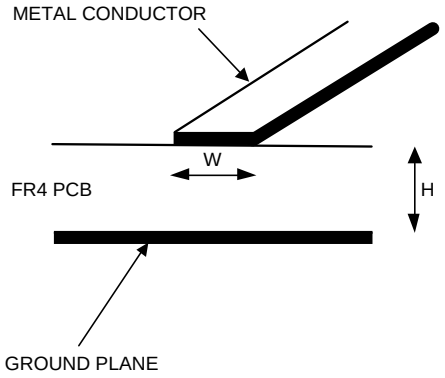


**Figure 95. Microstrip Configuration**

A conductor (trace) is placed on the topside of a PCB. The bottom side of the PCB has a fully copper ground plane. The characteristic impedance of the microstrip transmission line is a function of the width W, height H, and the dielectric constant $\varepsilon_r$.

Characteristics such as height and the dielectric constant of the board have significant impact on transmission line dimensions. A 50Ω transmission line may result in impractically wide traces. A typical 1.6 mm thick FR4 board results in a trace width of 2.9 mm, for instance. This is impractical for the LMH2100, since the pad width of the 6-Bump DSBGA package is 0.24 mm. The transmission line has to be tapered from 2.9 mm to 0.24 mm. Significant reflections and resonances in the frequency transfer function of the board may occur due to this tapering.

## GCPW Configuration

A transmission line in a (grounded) coplanar waveguide (GCPW) configuration will give more flexibility in terms of trace width. The GCPW configuration is constructed with a conductor surrounded by ground at a certain distance, S, on the top side. Figure 96 shows a cross section of this configuration. The bottom side of the PCB is a ground plane. The ground planes on both sides of the PCB should be firmly connected to each other by multiple vias. The characteristic impedance of the transmission line is mainly determined by the width W and the distance S. In order to minimize reflections, the width W of the center trace should match the size of the package pad. The required value for the characteristic impedance can subsequently be realized by selection of the proper gap width S.

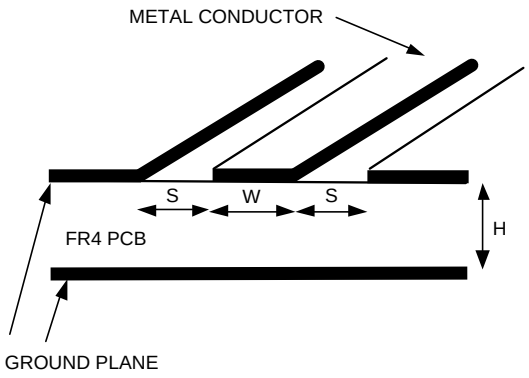


**Figure 96. GCPW Configuration**

### Reference REF

The Reference pin can be used to compensate for temperature drift of the internal reference voltage as described in Interface to the ADC. The REF pin is directly connected to the inverting input of the transimpedance amplifier. Thus, RF signals and other spurious signals couple directly through to the output. Introduction of RF signals can be prevented by connecting a small capacitor between the REF pin and ground. The capacitor should be placed close to the REF pin as depicted in Figure 94.

### Output OUT

The OUT pin is sensitive to crosstalk from the RF input, especially at high power levels. The ESD diode between the output and $V_{DD}$ may rectify the crosstalk, but may add an unwanted inaccurate DC component to the output voltage.

The board layout should minimize crosstalk between the detectors input $RF_{IN}$ and the detectors output. Using an additional capacitor connected between the output and the positive supply voltage ($V_{DD}$ pin) or GND can prevent this. For optimal performance this capacitor should be placed as close as possible to the OUT pin of the LMH2100.

## REVISION HISTORY

| Changes from Revision A (March 2013) to Revision B | Page |
|---|---|
| • Changed layout of National Data Sheet to TI format | 37 |

## PACKAGING INFORMATION

| Orderable Device | Status (1) | Package Type | Package Drawing | Pins | Package Qty | Eco Plan (2) | Lead/Ball Finish | MSL Peak Temp (3) | Op Temp (°C) | Top-Side Markings (4) | Samples |
|---|---|---|---|---|---|---|---|---|---|---|---|
| LMH2100TM/NOPB | ACTIVE | DSBGA | YFQ | 6 | 250 | Green (RoHS & no Sb/Br) | SNAGCU | Level-1-260C-UNLIM | -40 to 85 | J | Samples |
| LMH2100TMX/NOPB | ACTIVE | DSBGA | YFQ | 6 | 3000 | Green (RoHS & no Sb/Br) | SNAGCU | Level-1-260C-UNLIM | -40 to 85 | J | Samples |

(1) The marketing status values are defined as follows:
**ACTIVE:** Product device recommended for new designs.
**LIFEBUY:** TI has announced that the device will be discontinued, and a lifetime-buy period is in effect.
**NRND:** Not recommended for new designs. Device is in production to support existing customers, but TI does not recommend using this part in a new design.
**PREVIEW:** Device has been announced but is not in production. Samples may or may not be available.
**OBSOLETE:** TI has discontinued the production of the device.

(2) Eco Plan - The planned eco-friendly classification: Pb-Free (RoHS), Pb-Free (RoHS Exempt), or Green (RoHS & no Sb/Br) - please check http://www.ti.com/productcontent for the latest availability information and additional product content details.
**TBD:** The Pb-Free/Green conversion plan has not been defined.
**Pb-Free (RoHS):** TI's terms "Lead-Free" or "Pb-Free" mean semiconductor products that are compatible with the current RoHS requirements for all 6 substances, including the requirement that lead not exceed 0.1% by weight in homogeneous materials. Where designed to be soldered at high temperatures, TI Pb-Free products are suitable for use in specified lead-free processes.
**Pb-Free (RoHS Exempt):** This component has a RoHS exemption for either 1) lead-based flip-chip solder bumps used between the die and package, or 2) lead-based die adhesive used between the die and leadframe. The component is otherwise considered Pb-Free (RoHS compatible) as defined above.
**Green (RoHS & no Sb/Br):** TI defines "Green" to mean Pb-Free (RoHS compatible), and free of Bromine (Br) and Antimony (Sb) based flame retardants (Br or Sb do not exceed 0.1% by weight in homogeneous material)

(3) MSL, Peak Temp. -- The Moisture Sensitivity Level rating according to the JEDEC industry standard classifications, and peak solder temperature.

(4) Multiple Top-Side Markings will be inside parentheses. Only one Top-Side Marking contained in parentheses and separated by a "~" will appear on a device. If a line is indented then it is a continuation of the previous line and the two combined represent the entire Top-Side Marking for that device.

## TAPE AND REEL INFORMATION

**REEL DIMENSIONS**

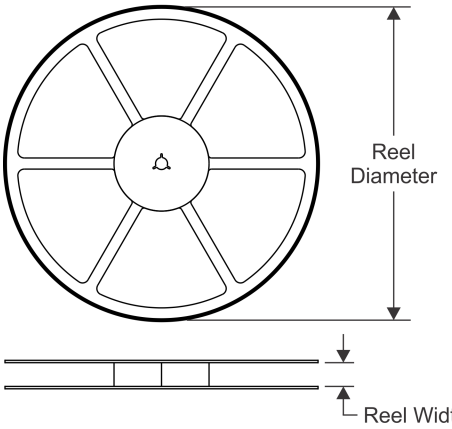


**TAPE DIMENSIONS**

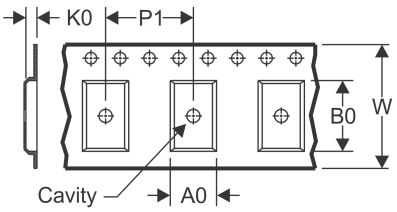


| | |
|---|---|
| A0 | Dimension designed to accommodate the component width |
| B0 | Dimension designed to accommodate the component length |
| K0 | Dimension designed to accommodate the component thickness |
| W | Overall width of the carrier tape |
| P1 | Pitch between successive cavity centers |

**QUADRANT ASSIGNMENTS FOR PIN 1 ORIENTATION IN TAPE**

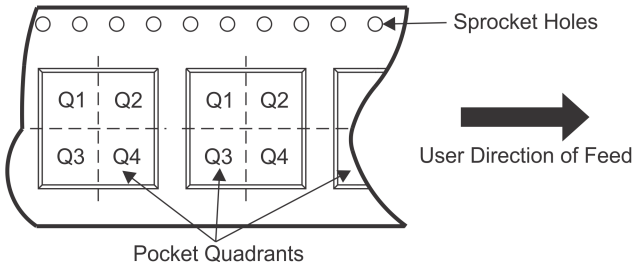


*All dimensions are nominal

| Device | Package Type | Package Drawing | Pins | SPQ | Reel Diameter (mm) | Reel Width W1 (mm) | A0 (mm) | B0 (mm) | K0 (mm) | P1 (mm) | W (mm) | Pin1 Quadrant |
|---|---|---|---|---|---|---|---|---|---|---|---|---|
| LMH2100TM/NOPB | DSBGA | YFQ | 6 | 250 | 178.0 | 8.4 | 0.89 | 1.3 | 0.7 | 4.0 | 8.0 | Q1 |
| LMH2100TMX/NOPB | DSBGA | YFQ | 6 | 3000 | 178.0 | 8.4 | 0.89 | 1.3 | 0.7 | 4.0 | 8.0 | Q1 |

TAPE AND REEL BOX DIMENSIONS

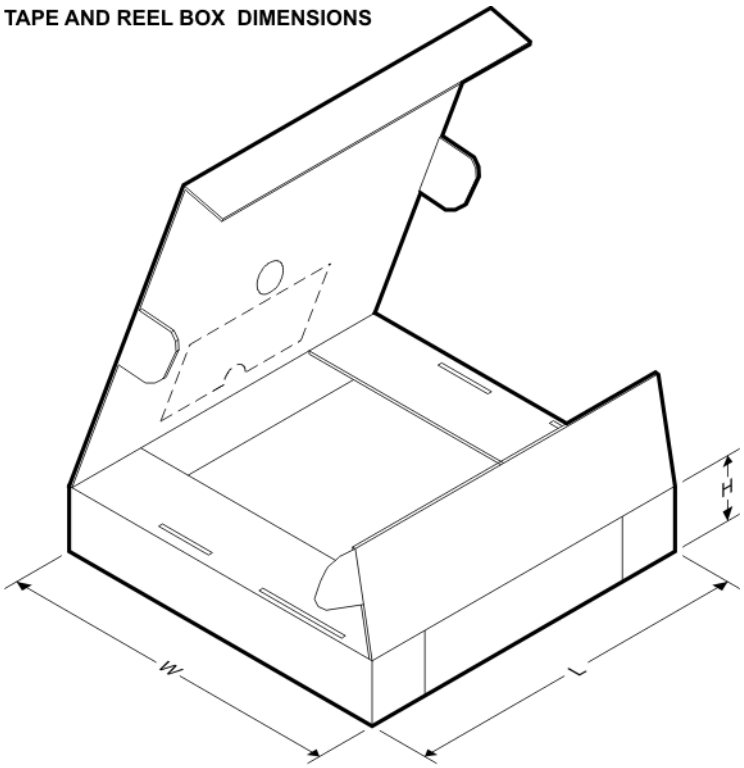


*All dimensions are nominal

| Device | Package Type | Package Drawing | Pins | SPQ | Length (mm) | Width (mm) | Height (mm) |
|---|---|---|---|---|---|---|---|
| LMH2100TM/NOPB | DSBGA | YFQ | 6 | 250 | 210.0 | 185.0 | 35.0 |
| LMH2100TMX/NOPB | DSBGA | YFQ | 6 | 3000 | 210.0 | 185.0 | 35.0 |

# YFQ0006

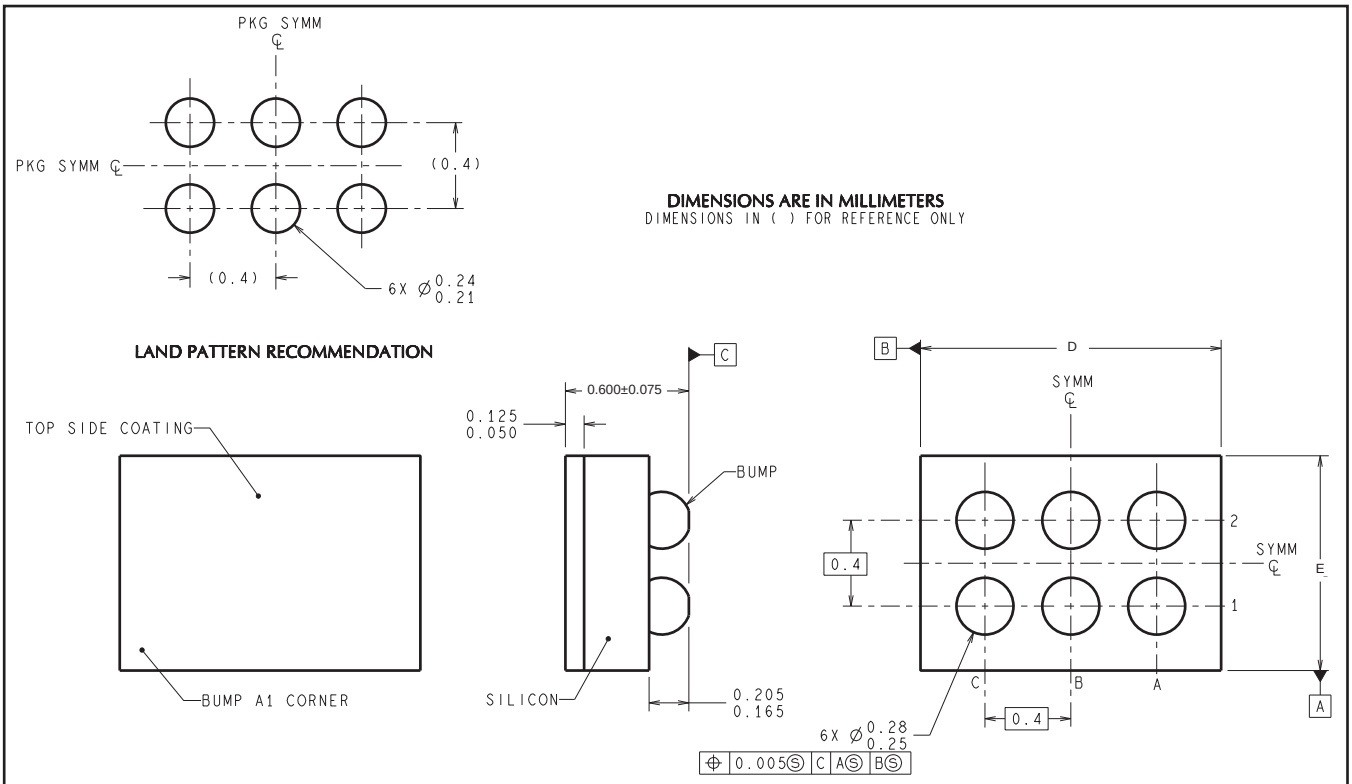


D: Max = 1.274 mm, Min =1.214 mm

E: Max = 0.874 mm, Min =0.814 mm

4215075/A 12/12

NOTES: A. All linear dimensions are in millimeters. Dimensioning and tolerancing per ASME Y14.5M-1994.
B. This drawing is subject to change without notice.

## IMPORTANT NOTICE

Texas Instruments Incorporated and its subsidiaries (TI) reserve the right to make corrections, enhancements, improvements and other changes to its semiconductor products and services per JESD46, latest issue, and to discontinue any product or service per JESD48, latest issue. Buyers should obtain the latest relevant information before placing orders and should verify that such information is current and complete. All semiconductor products (also referred to herein as “components”) are sold subject to TI’s terms and conditions of sale supplied at the time of order acknowledgment.

TI warrants performance of its components to the specifications applicable at the time of sale, in accordance with the warranty in TI’s terms and conditions of sale of semiconductor products. Testing and other quality control techniques are used to the extent TI deems necessary to support this warranty. Except where mandated by applicable law, testing of all parameters of each component is not necessarily performed.

TI assumes no liability for applications assistance or the design of Buyers’ products. Buyers are responsible for their products and applications using TI components. To minimize the risks associated with Buyers’ products and applications, Buyers should provide adequate design and operating safeguards.

TI does not warrant or represent that any license, either express or implied, is granted under any patent right, copyright, mask work right, or other intellectual property right relating to any combination, machine, or process in which TI components or services are used. Information published by TI regarding third-party products or services does not constitute a license to use such products or services or a warranty or endorsement thereof. Use of such information may require a license from a third party under the patents or other intellectual property of the third party, or a license from TI under the patents or other intellectual property of TI.

Reproduction of significant portions of TI information in TI data books or data sheets is permissible only if reproduction is without alteration and is accompanied by all associated warranties, conditions, limitations, and notices. TI is not responsible or liable for such altered documentation. Information of third parties may be subject to additional restrictions.

Resale of TI components or services with statements different from or beyond the parameters stated by TI for that component or service voids all express and any implied warranties for the associated TI component or service and is an unfair and deceptive business practice. TI is not responsible or liable for any such statements.

Buyer acknowledges and agrees that it is solely responsible for compliance with all legal, regulatory and safety-related requirements concerning its products, and any use of TI components in its applications, notwithstanding any applications-related information or support that may be provided by TI. Buyer represents and agrees that it has all the necessary expertise to create and implement safeguards which anticipate dangerous consequences of failures, monitor failures and their consequences, lessen the likelihood of failures that might cause harm and take appropriate remedial actions. Buyer will fully indemnify TI and its representatives against any damages arising out of the use of any TI components in safety-critical applications.

In some cases, TI components may be promoted specifically to facilitate safety-related applications. With such components, TI’s goal is to help enable customers to design and create their own end-product solutions that meet applicable functional safety standards and requirements. Nonetheless, such components are subject to these terms.

No TI components are authorized for use in FDA Class III (or similar life-critical medical equipment) unless authorized officers of the parties have executed a special agreement specifically governing such use.

Only those TI components which TI has specifically designated as military grade or “enhanced plastic” are designed and intended for use in military/aerospace applications or environments. Buyer acknowledges and agrees that any military or aerospace use of TI components which have ***not*** been so designated is solely at the Buyer's risk, and that Buyer is solely responsible for compliance with all legal and regulatory requirements in connection with such use.

TI has specifically designated certain components as meeting ISO/TS16949 requirements, mainly for automotive use. In any case of use of non-designated products, TI will not be responsible for any failure to meet ISO/TS16949.

| **Products** | | **Applications** | |
|---|---|---|---|
| Audio | www.ti.com/audio | Automotive and Transportation | www.ti.com/automotive |
| Amplifiers | amplifier.ti.com | Communications and Telecom | www.ti.com/communications |
| Data Converters | dataconverter.ti.com | Computers and Peripherals | www.ti.com/computers |
| DLP® Products | www.dlp.com | Consumer Electronics | www.ti.com/consumer-apps |
| DSP | dsp.ti.com | Energy and Lighting | www.ti.com/energy |
| Clocks and Timers | www.ti.com/clocks | Industrial | www.ti.com/industrial |
| Interface | interface.ti.com | Medical | www.ti.com/medical |
| Logic | logic.ti.com | Security | www.ti.com/security |
| Power Mgmt | power.ti.com | Space, Avionics and Defense | www.ti.com/space-avionics-defense |
| Microcontrollers | microcontroller.ti.com | Video and Imaging | www.ti.com/video |
| RFID | www.ti-rfid.com | | |
| OMAP Applications Processors | www.ti.com/omap | **TI E2E Community** | e2e.ti.com |
| Wireless Connectivity | www.ti.com/wirelessconnectivity | | |

Mailing Address: Texas Instruments, Post Office Box 655303, Dallas, Texas 75265